METEOR-Berichte

Role of Eddies in the Carbon Pump of Eastern Boundary Upwelling Systems, REEBUS

Cruise No. M156

03.07. – 01.08.2019
Mindelo (Cap Verde) – Mindelo

Stefan Sommer, Nicole Adam, Kevin Becker, Andrew W. Dale, Johannes Hahn, Mareike Kampmeier, Melf Paulsen, Sven Katzenmeier, Arne Körtzinger

Chief Scientist Stefan Sommer
GEOMAR Helmholtz Centre for Ocean Research Kiel

2020

Table of Contents

1 Summary

The major goal of the RV METEOR cruise M156 to Cape Verdian waters and the Mauritanian upwelling area off West Africa was to contribute to a better quantitative understanding of the effects of mesoscale eddies on CO_2 source/sink mechanisms and the biological carbon pump in eastern boundary upwelling areas as well as their effects to the oligotrophic periphery including the deep-sea floor. The cruise M156 (MOSES Eddy Study I) was conducted within the framework of the BMBF funded REEBUS project (Role of Eddies in the Carbon Pump of Eastern Boundary Upwelling Systems) by a consortium of physical, biological (benthic microbiology, bacterial plankton, protists) and biogeochemical oceanographers. Specific aims were **i.** the quantification of solute and particle fluxes within and at the periphery of eddies; **ii.** to determine the turnover of carbon species, air-sea gas exchange of CO_2, **iii.** the determination of the protistan and bacterial plankton community structures in the surface layers of an eddy, and **iv.** to quantify the magnitude and variability of material fluxes to the seabed and turnover in the sediment underneath the eddy passage. To achieve these aims, the cruise had two major observing strategies: i. an intense benthic/pelagic program along the zonal eddy passage at 18°N. Along this corridor ranging from 24°20' to 16°30'W, five benthic/pelagic stations (E1 to E5) in different water depths and distances from the Mauritanian coast were performed. The motivation for this survey has been to resolve zonal gradients in pelagic element cycling as well as of organic matter degradation and burial in the seabed, which in turn could potentially be linked with changes in eddy induced primary- and export production. ii. the detailed investigation of an individual eddy to investigate physical, biogeochemical and biological processes on meso- to submeso-scales (100km to 10m). Satellite data analysis was performed before and during the cruise to identify a suitable eddy from a combination of sea-level anomaly, ocean color as Chl-a proxy, and sea-surface temperature supplemented with shipboard current velocity measurements.
A total of 171 stations were sampled. The water column program consists of 59 CTD casts, 29 MSS and 20 Marine Snow Catcher deployments. For biogeochemical measurements at the sea surface two deployments of a Lagrangian Surface Drifter and one Waveglider deployment were conducted. At the seafloor, we conducted 10 BIGO deployments. Ten seafloor imaging surveys were performed using the towed camera system OFOS, supplemented with 7 Multibeam and 1 Sidescan surveys. In deviation from the cruise proposal, the planned long-term deployment of a Lander, which was planned to record a time series of oxygen fluxes during the passage of an eddy, was not deployed due to a major delay in its design and manufacturing. The planned AUV (Girona 500) deployments at the shallow E5 station close to the Mauritanian coast station did also not take place. Despite moderate weather conditions, all deployments were successful, hence all the data and sample material aimed for has been achieved. It is to expect that as planned all scientific questions can be addressed. Especially in the synthesis of all REEBUS cruises and the consideration of data from earlier cruises (MSM17/4, M107) into this region a high scientific potential can be expected.

Zusammenfassung

Die Hauptzielsetzung der METEOR Expedition M156 zu den Kap Verden und dem Auftriebsgebiet vor Mauretanien ist es ein besseres Verständnis der Auswirkungen von mesoskaligen Wirbeln auf Quellen und Senken Mechanismen von Kohlendioxid und der biologischen Kohlenstoffpumpe in Auftriebsgebieten zu bekommen. Dies umfasst ferner die Auswirkung von Wirbeln auf deren nährstoffarme Umgebung sowie den Kohlenstoffumsatz des Tiefseebodens. Die Forschungsreise M156 (MOSES Eddy Study I) wurde innerhalb des vom BMBF geförderten REEBUS Projekts (Role of Eddies in the Carbon Pump of Eastern Boundary Upwelling Systems) von einem wissenschaftlichen Team bestehend aus physikalischen, biologischen (benthische Mikrobiologie, bacterielle Planktologie, Protozoologie) und biogeochemischen Ozeanographen durchgeführt. Spezifische Ziele waren **i.** die Erfassung von Flüssen von Partikeln und gelöster Substanzen

innerhalb und an der Peripherie eines Wirbels, **ii.** die Erfassung des Umsatzes von organischem Kohlenstoff und des CO_2 Austausches entlang der Wasser-Atmosphären Grenzschicht, **iii.** die Erfassung der Lebensgemeinschaften von Protozoen und des bakteriellen Planktons in den Oberflächenschichten eines Wirbels, und **iv.** die Quantifizierung von Stoffflüssen entlang der Sediment-Wassergrenzschicht und des Stoffumsatzes im Meeresboden unterhalb der Wirbelpassage. Das Arbeitsprogramm umfasste zum einen ein benthisch/pelagisches Messprogramm entlang der zonalen Wirbelpassage bei 18°N. Entlang dieses Korridors, der sich von 24°20' bis 16°30'W erstreckte wurden 5 benthisch-pelagische Stationen (E1 bis E5) in verschiedenen Wassertiefen und Entfernungen zur Mauretanischen Küste beprobt. Die Motivation für diese Messungen war die Erfassung von zonalen Gradienten des pelagischen Kohlenstoffs und dessen Umsatz sowie die Erfassung des Organik-Abbaus in den darunterliegenden Sedimenten und diese mit der Primärproduktion an der Meeresoberfläche in Bezug zu setzen. Ferner wurde ein detailliertes Messprogramm eines einzelnen Wirbels durchgeführt um physikalische, biogeochemische und biologische Prozesse auf Meso- und Submesoskalen (100km bis 10m) zu erfassen. Die Identifikation eines geeigneten Wirbels erfolgte vor und während der Reise anhand von Satellitenbeobachtungen (Meeresspiegelanomalie, Chl.a Gehalt, Meeresoberflächen-Temperatur) in Verbindung mit Strömungsdaten, die an Bord erhoben wurden.
Insgesamt wurden 171 Stationen beprobt. Das Arbeitsprogramm in der Wassersäule umfasste 59 CTD, 29 Mikro-Struktur CTD und 20 Marine Snow Catcher Einsätze. Zu biogeochemischen Messungen an der Meeresoberfläche wurde zweimal der Lagrangian Surface Drifter und einmal ein Waveglider eingesetzt. Am Meeresboden erfolgten 10 Verankerungen des BIGO Landers und 10 Videokartierungen mittels des geschleppten Kamera-Sensorik Systems OFOS, die durch 7 Multibeam und 1 Sidescan Einsätze ergänzt wurden. Abweichend vom Fahrtantrag konnte die geplante Langzeit-Verankerung eines Landers zur Zeitserienerfassung der Sauerstoffaufnahme von Sedimenten während der Passage eines Wirbels nicht durchgeführt werden, da es zu Verzögerungen bei dessen Fertigung kam. Ebenfalls konnten die AUV-Einsätze (Girona 500) an der flachen Station E5 vor Mauretanien nicht durchgeführt werden. Trotz moderater Wetterbedingungen gab es keine schwerwiegenden Probleme beim Geräteeinsatz, die das wissenschaftliche Programm hätten gefährden können. Es ist daher zu erwarten, dass wie geplant alle wissenschaftlichen Fragestellungen adressiert werden können. Hierbei liegt in der Synthese der Datensätze aller REEBUS Reisen, sowie die Einbeziehung von Daten der früheren Ausfahrten MSM17/4 und M107 in diese Region ein hohes wissenschaftliches Potential.

2 Participants

2.1 Prinicpal Investigators

Name	Institution
Dr. Sommer, S.	GEOMAR
Adam, N.	GEOMAR
Dr. Becker, K.	GEOMAR
Breiner, H.W.	TU KL
Dr. Dale, A.W.	GEOMAR
Kampmeier, M.	GEOMAR
Dr. Hahn, J.	GEOMAR
Paulsen, M.	GEOMAR

2.2 Cruise Participants

	Name	Discipline	Institution
1.	Dr. Sommer, Stefan	PI, Lander, Geochemistry	GEOMAR
2.	Adam, Nicole	Microbiology	GEOMAR
3.	Dr. Becker, Kevin	Pelagic Biogeochemistry	GEOMAR
4.	Bill, Nicolas	Geochemistry	GEOMAR
5.	Breiner, Hans-Werner	Protozoan Biology	TU KL
6.	Bunsen, Frauke	Physical Oceanography	GEOMAR
7.	Dr. Dale, Andrew	Geochemistry	GEOMAR
8.	Devresse, Quentin	Pelagic Biogeochemistry	GEOMAR
9.	Dr. Dilmahamod A. Fehmi	Physical Oceanography	GEOMAR
10.	Domeyer, Bettina	Geochemistry	GEOMAR
11.	El Abed, Jemal	Observer	IMROP
12.	Dr. Hahn, Johannes	Physical Oceanography	GEOMAR
13.	Kampmeier, Mareike	Seafloor Monitoring	GEOMAR
14.	Katzenmeier, Sven	Protozoan Biology	TU KL
15.	Klüver, Tanja	Pelagic Biogeochemistry	GEOMAR
16.	Link, Rudolph	Physical Oceanography	GEOMAR
17.	Paulsen, Melf	Pelagic Biogeochemistry	GEOMAR
18.	Petersen, Asmus	Lander Mechanics	GEOMAR
19.	Dr. Rickert, Esther	Pelagic Biogeochemistry	GEOMAR
20.	Roa, Jon	Pelagic Biogeochemistry	GEOMAR
21.	Rudloff, Daniel	Physical Oceanography	GEOMAR
22.	Scheidemann, Lindsay	Pelagic Biogeochemistry	GEOMAR
23.	Schmidt, Thilo	Geochemistry	GEOMAR
24.	Schott, Thorsten	Seafloor Monitoring	GEOMAR
25.	Schüssler, Gabriele	Microbiology	GEOMAR
26.	Schumacher, Mia	Seafloor Monitoring	GEOMAR
27.	Stelzner, Martin	Bordwetterwarte	DWD
28.	Surberg, Regina	Microbiology	GEOMAR
29.	Türk, Matthias	Lander Electronics	GEOMAR

2.3 Participating Institutions

Name	Institution
GEOMAR	Helmholtz-Zentrum für Ozeanforschung Kiel Wischhofstrasse 1-3, 24148 Kiel, Germany, E-mail: ssommer@geomar.de
TU KL	University of Kaiserslautern, Faculty of Biology, Department of Ecology, Gottlieb-Daimler-Str. Building 14, 67663 Kaiserslautern, Germany
IMROP	Institut Mauritanien de Recherche Océanographiques et des Pêches, Nouakchott, Mauritania
DWD	Deutscher Wetterdienst Geschäftsfeld Seeschifffahrt Bernhard-Nocht-Straße 76 20359 Hamburg / Germany e-mail: seeschifffahrt@dwd.de Internet: www.dwd.de

3 Research Program

3. 1 Aims of the Cruise

The overarching goal of the RV METEOR cruise M156 to the Mauritanian upwelling area off West Africa and Cape Verde was to obtain a better quantitative understanding of the dynamics of mesoscale eddies with particular focus to CO_2 source/sink mechanisms and the biological carbon pump in eastern boundary upwelling areas as well as their effects to the oligotrophic periphery including the deep-sea floor. By trapping coastal waters of upwelling origin and transporting them westwards into the open ocean, eddies play an important role in the lateral mixing and transport of physical-biogeochemical properties and thereby modulate biological productivity and material fluxes to the seabed. The cruise is embedded into a series of three REEBUS cruises.
Specific aims of the different working groups were as follows:

Physical oceanography

- Determine the spatial and temporal variability of eddy-associated mixing processes and quantify diapycnal fluxes of solutes and particles within and at the periphery of eddies;
- Investigate internal wave - eddy interactions and its contribution to elevated mixing within and at the periphery of eddies.

Pelagic biogeochemistry

- Assess vertical and horizontal transport pathways of different carbon species in and around different eddy types and life stages;
- Estimate the air-sea gas exchange of CO_2 as well as net community production and oxygen utilization in the surface and subsurface layer at different life stages of eddies;
- Determine the production and microbial utilization of dissolved and non-sinking organic matter to estimate nutrient remineralization and microbial CO_2 fluxes in different eddy types. Deliver a high-resolution description of vertical concentration gradients for a variety of DOM components and for non-sinking organic matter, (transparent exopolymer particles (TEP), coomassie stainable particles (CSP)) and bacteria; assess the potential utility of chromophoric DOM and fluorescent DOM components as tracers for eddy dynamics and vertical DOC fluxes; evaluate the potential biological availability of DOM in surface and OMZ waters based on molecular compound analysis and bio-assays;
- Estimate primary production, exudation and heterotrophic recycling as well as respiration of organic matter within and around eddies.

Biological Oceanography

- Analyses of protistan and bacterial plankton community structures and species turnover patterns in relation to eddy dynamics on vertical and horizontal scales using DNA metabarcoding;
- Conduct shipboard experiments to assess the effect of eddies on microplankton biomass and community assemblages;
- Determine benthic microbial community structures and species turnover patterns alongside the zonal eddy corridor. While DNA metabarcoding will allow the proportion of inactive organisms sinking down from the water column to be identified, RNA metabarcoding will identify the indigenous part of the benthic microbial communities.

Benthic biogeochemistry and geology

- Quantify the rain rate of organic matter to the seabed and organic matter burial in sediments underneath the eddy passage;
- Decipher the origin of organic matter reaching the seabed (shelf versus open ocean);
- map the regional distribution of benthic organic matter fluxes alongside the zonal eddy corridor.

3.2 Agenda of the Cruise and description of the work area

As outlined in the cruise proposal the above objectives were approached by two major observing objectives. **The first observing objective** was a benthic/pelagic program within the zonal eddy passage at 18°, Figures 3.2.1, 3.2.2. Along this corridor, five benthic stations (E1 to E5) in different water depths and distances from coast of Cape Verde and Mauritania were sampled. We slightly deviated from the planned positions provided in the cruise proposal to allow for a better comparison with data from previous cruises. This survey enabled investigating zonal gradients in organic matter degradation and burial in the seabed, which in turn could potentially be linked with changes in eddy primary- and export production. In between the main E stations further side stations (S) were sampled for water column hydrographic and biogeochemical measurements. In addition to the zonal depth transect a further station (CB) closely located to Cape Blanc was sampled, as this site has been constantly surveyed with sediment traps over the last two decades (Fischer et al. 2016). This allows the interpretation benthic-pelagic measurements in relation to the CB mass flux records.

At these stations an intense biological (microbiology, protozoology), biogeochemical and physical working program was conducted (for details see below). The water column was sampled using the CTD water sampling rosette, a Marine Snow Catcher for particle analysis, and a microstructure probe for turbulence measurements. The shipboard ADCP for current measurements was in operation during the entire time course of the cruise.

At each of these main stations benthic element turnover was investigated using two BIGO type lander (Biogeochemical Observatory, BIGO-I and BIGO-II), each quipped with two benthic flux chambers for in situ flux measurements of oxygen and other major solutes. The in-situ flux measurements were complemented with microbiological investigations and biogeochemical pore water and solid phase analyses using a video controlled Multiple Corer (MUC) for sediment retrieval. At the benthic sampling-sites intense seafloor monitoring was conducted using the towed camera system OFOS (Ocean Floor Observation System). Bathymetrical measurements using the shipboard multibeam system complemented the sea floor investigations.

The second observing objective has been the detailed investigation of an individual eddy to investigate physical, biogeochemical and biological cycling and transport processes on meso- to submeso-scales (100km to 10m). Satellite data analysis was performed before and during the cruise to identify a suitable eddy from a combination of altimetry, ocean color (Chl-a proxy), and sea-surface temperature data supplemented with shipboard current velocity measurements. During the time course of the cruise the center of the cyclonic eddy was incrementally better constrained

and water column sampling of the eddy took place along the zonal transect EDZ and the meridional transects EDM and EDM_E, Figure 3.2.2 and 3.2.3. In Figure 3.2.3 the approximate position of the eddy is indicated by blue contour lines. The sampling of the water colum took place using the instruments mentioned above including a Waveglider for the measurement of the physical and biogeochemical properties at the sea surface, a Glider (physical properties, turbulence, O_2, nitrate), and a Lagrangian Surface Drifter (biogeochemical properties). The objectives are to obtain a comprehensive, multidisciplinary picture of physical, biogeochemical and biological characteristics of the eddy. Dynamical pathways will be compared to the water characteristics at the eddy generation site or outside the eddy.

At the seafloor encompassing water depths of about 2700 to 3000 m likely effects of eddy induced enhanced export production on benthic carbon processing were investigated using the BIGO type lander complemented with sediment biogeochemical analyses using the MUC for sediment retrieval (Fig. 3.2.3). A specific lander (BBL) was placed at the southern periphery of the cyclone for sea floor imaging and the measurement of physical properties (Fig. 3.2.3). As already described above the sea floor imaging (OFOS) and bathymetrical measurements were conducted. Side scan imaging for the detailed recognition of specific sea floor features was preformed along a transect through the projected eddy area.

Overall, we conducted 59 CTD casts, 29 MSS deployments, 20 Marine Snow Catcher deployments, two deployments of the Lagrangian Surface Drifter and one Waveglider deployment. At the seafloor, we conducted 10 BIGO deployments, one of which at station E1 failed. We were not able to repeat this deployment due to time constraints. Overal 10 OFOS surveys were performed supplemented with 7 Multibeam and 1 Sidescan surveys. The BBL lander as deployed once. Overall, a total of 171 stations were conducted.

Apart from minor shifts in the positions the measurement campaign was conducted as outlined in the cruise proposal. Except minor technological complications with the BIGO lander, there were no major failures, which could have endangered the scientific success of the research cruise.

However, two technological issues should be mentioned. Firstly, the Einstein Lander, which was planned to record a time series of oxygen fluxes during the passage of an eddy, was not deployed. Technological problems and a lack of personnel caused a major delay in the design and manufacturing of this platform. This Lander would have been necessary to record changes of oxygen fluxes in response to changing export production during the passage of eddies at the sea surface. The design of an early version of the stationary lander type platform has been abandoned in favor of a mobile Rover, which is presently manufactured at GEOMAR. Its deployment is planned for the 3rd REEBUS/MOSES cruise in October/November 2021, to be recovered in late 2022. The planned AUV deployments (Girona 500) at the shallow site E5 close to the Mauritanian coast did not take place for technological reasons.

According to the ship time proposal, we successfully conducted measurements at all planned stations. We followed the DFG regulations summarized in the „Erklärung zu einer verantwortungsvollen Meeresforschung“ and the (OSPAR) Code „Code of Conduct for Responsible Marine Research in the Deep Seas and High Seas of the OSPAR Maritime Area” to avoid unnecessary environmental and ecosystem disturbances. The impact of the conducted work to the environment can be considered as very minor. All lander were recovered. There were no activities, which could lead to substantial physical, chemical, biological or geological changes or damage of marine habitats. Care was taken to avoid activities, which could disturb the experiments and observations of other scientists. We made use of the most environmentally-friendly and appropriate study methods, which are presently available, and avoided collections that are not essential to conduct the scientific research. The number of samples was reduced to the necessary minimum.

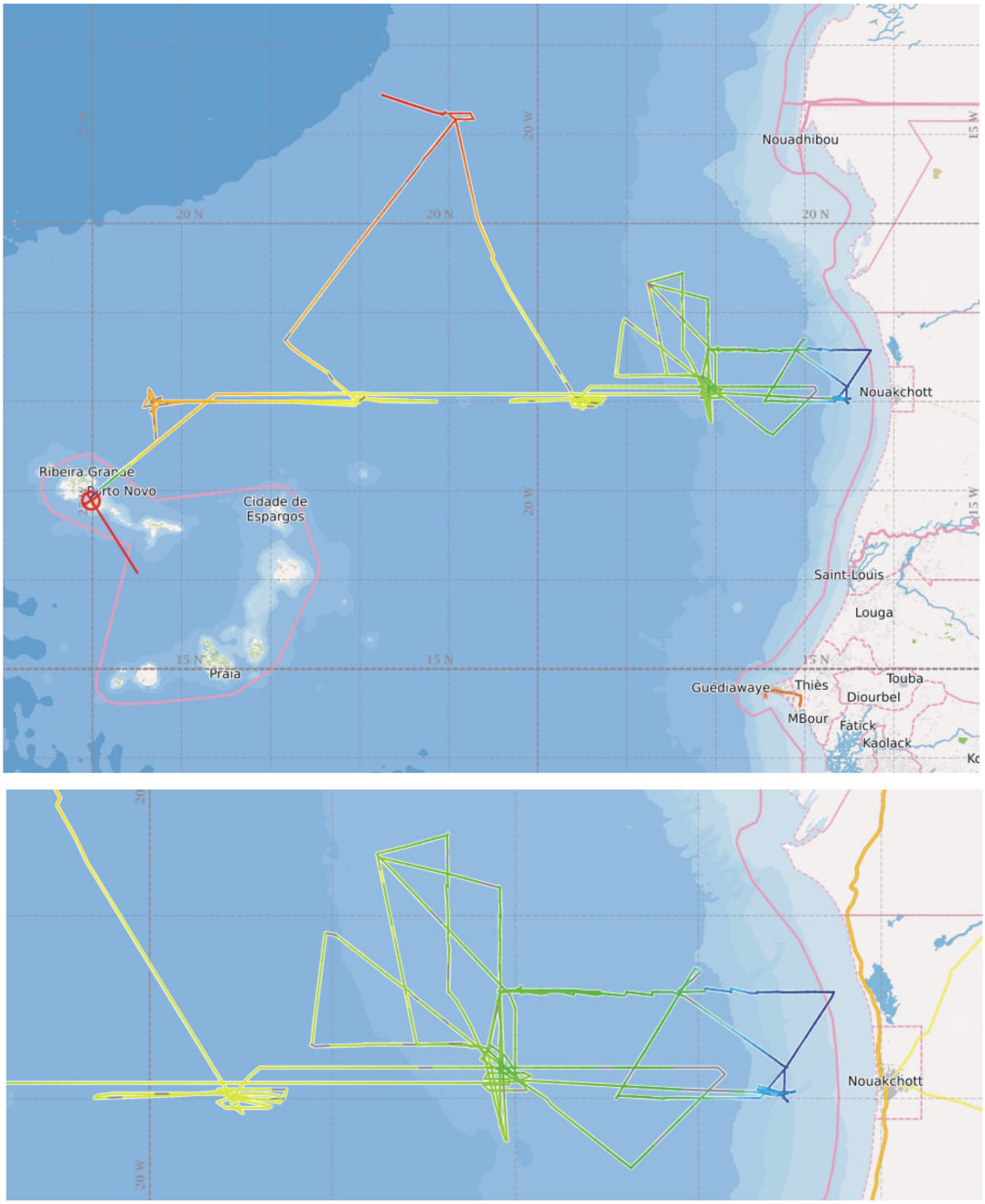

Fig. 3.2.1 Track plot of the cruise M156 off Cape Verde and Mauritania. The cruise started and ended in Mindelo.

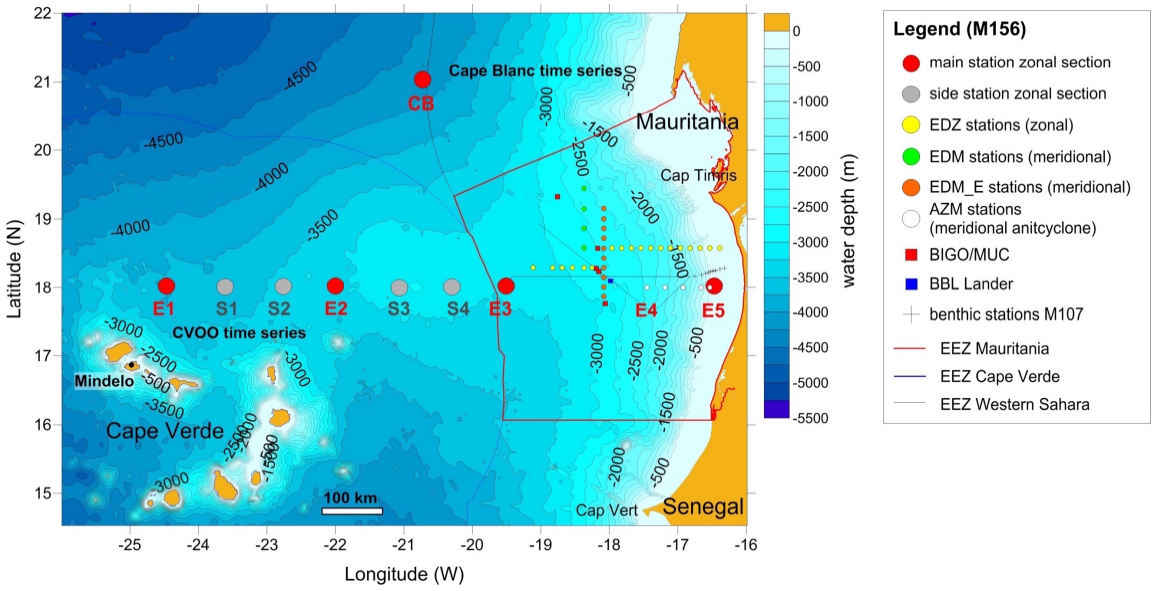

Fig. 3.2.2: Detailed station map of the sampling scheme during R/V METEOR cruise M156.

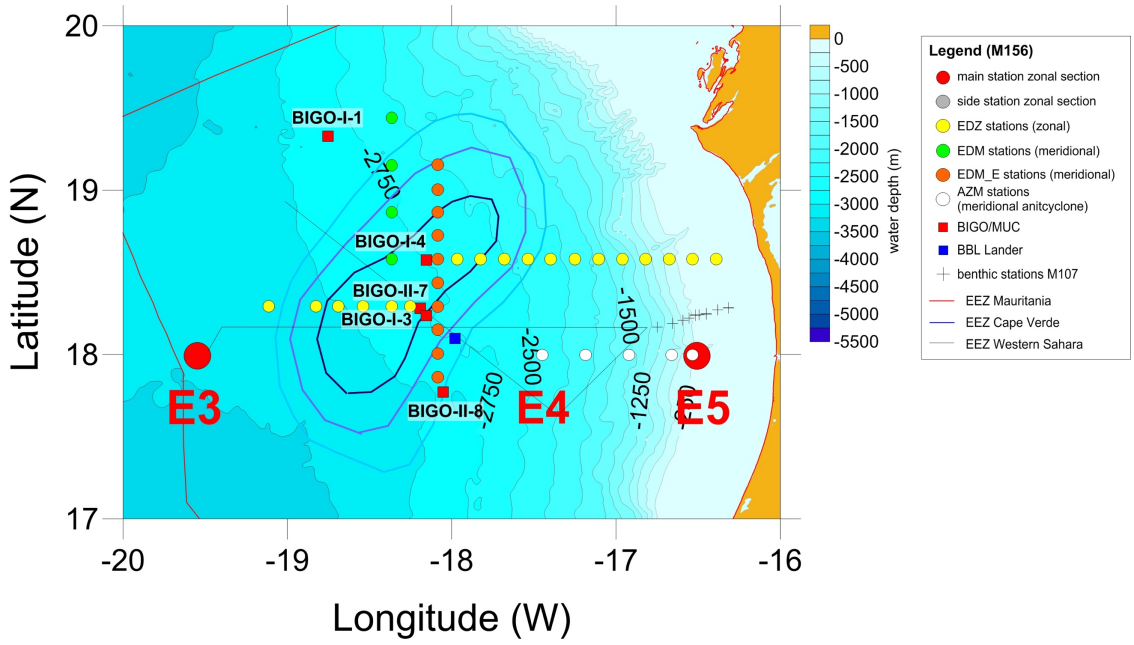

Fig. 3.2.3: Regional sampling scheme of the cyclonic eddy (indicated by blue contours) off Mauritania.

4 Narrative of the cruise

The working program of the cruise was based on two major observing objectives. The first objective was an intense benthic/pelagic sampling program within the zonal eddy passage at 18°N. This corridor, included five main stations (E1 to E5) in different water depths and distances from the Mauritanian coast. The stations were investigated to reveal zonal gradients in organic matter degradation and burial in the seabed, which in turn could potentially be linked with changes in eddy primary- and export production. In between the main stations side stations were specified for further biological and biogeochemical water column investigations. Beside the 18°N section

another main station was located further north (21°10'N 20°55'W) close to the Cap Blanc time series station (CB) at a water depth of about 4190 m. For this site an extended data set of particle flux from the sea surface to seafloor is available and will help to interpret our in-situ flux measurements at the main stations E1 to E3. For the shallow station E5 in situ flux measurements became available during RV MERIAN cruise MSM17 and RV METEOR cruise M107 (both cruises were conducted within the Kiel SFB 754) and can be related to the measurements conducted during this cruise. The second observing objective represented the detailed investigation of an individual eddy to investigate physical, biogeochemical and biological processes.

On board was a diverse team of 29 scientists from 4 different institutions (GEOMAR Kiel, DWD, IMROP, TU Kaiserslautern), covering different disciplines including physical- and biogeochemical oceanography, microbiology, protozoology and sea floor monitoring.
During the day-time we typically deployed the Multiple Corer (MUC) to obtain undisturbed sediment cores and the two BIGO-type lander for in situ flux measurements at the seafloor. The benthic flux measurements comprise measurements of the total oxygen uptake, which is indicative for the carbon turnover as well as the exchange of nutrients inside the two flux chambers in each BIGO. Ex situ measurements on board of the RV METEOR included O_2 micro-profiling and incubation experiments to complement the benthic in-situ flux measurements. Onboard incubations were conducted to study the food web in the water column (TU KL), for microbiological rate measurements and respiration rate measurements in water column samples.
At night and during early morning hours, we typically deployed the CTD water sampling rosette (CTD) for the measurement of physical properties and nutrients, a Marine Snow Catcher (MSC) to retrieve particles from the water column, and a microstructure CTD (MSS) for turbulence measurements. We further deployed a Glider for autonomous and continuous measurements of physical parameters, currents, oxygen as well as nitrate. The water column investigations were complemented by the deployment of a Lagrangian surface drifter (LD) and a wave glider for biogeochemical measurements. Furthermore, seafloor imaging was conducted at each main station and the eddy site using the towed camera system OFOS (Ocean floor Observation System). The obtained images will be related to high resolution bathymetrical maps and side scan images. During all activities, the vessel mounted vmADCP was used for current measurements. A BBL Lander (Benthic Boundary Layer Lab) was deployed from the 22.07. to 30.07.19 southern periphery of the investigated eddy.

After finishing the investigations at E1 and E2 at the 09.07.2019, we headed towards an ADCP transect between positions ED-1 (18°40.5'N 22°50.57' W) and ED-2 (19°37.5'N 22°7.5'W), where currents along an anticyclonic eddy structure were measured. At the 10th of July, station work at the CB station started with the deployment of the BIGO Lander. At the beginning of the cruise we had severe problems to release the lander from the launching unit. Fortunately, we had the possibility to replace the electronic releaser with a conventional gas releaser, enabling successful lander deployment. Subsequently station work was continued with deployments of the CTD, MSC, MUC and seafloor mapping.
At Friday 12th of July we finished our station work at the CB station and headed south towards the station E3 at the 18°N zonal transect, where we arrived in the morning hours at the 13th of July and started with the deployment of the MUC. During the transit, we had a science meeting to discuss the details of the sampling strategy of the eddy.
Stationwork at E3 was finished at Monday 15th July after retrieval of the BIGO lander and we addressed the second observing objective of the cruise to study a cyclonic eddy in greater detail.

The location of the eddy was identified with support from scientists at GEOMAR (F. Heukamp, J. Karstensen, M. Dengler) who provided us with a daily update of satellite images allowing to locate a suitable eddy. The center the cyclonic eddy was at approximately 18°25'W - 18°05'W

and 18°30'N – 18°45'N (hereafter named as 18.5°W, 18°N cyclonic eddy) with a diameter (merdional distance between the two maxima of the current velocities at the eddy periphery) of about 1° (110 km). The extension of the eddy covered the main station E4 and several side stations whose positions in contrast to the original planning were shifted by 10 nm miles to the North. First activities, comprised current measurements along a transect across the eddy to better constrain its edges and center. At the 16th July, we conducted a 24 h side scan observation, which allowed us to determine the placement of the BIGO and BBL lander.
At the 20th July, we observed and sampled an open ocean red tide formed by the ciliate *Mesodinium rubrum*. Its occurrence was probably trigged by enhanced nutrient availability due to the deposition of Sahara dust, whether its occurrence can be further related to the eddy remains speculative. The intense investigation of the selected eddy continued until the 28th July. Subsequently, the RV METEOR headed towards the coastal main station E5. There station work further included several stations (AZM, cf. Figure 3.2.3) along a zonal transect through an anticyclonic eddy, which just developed close to the coast. At the 30th July, the RV METEOR travelled towards Mindelo (Cape Verde Islands). On our way back, the recovery of the BBL Lander and light measurements at the sea surface concluded the station work. During the entire cruise the weather conditions were fine allowing station work at all time.
We arrived in the harbour of Mindelo at the 1st of August at around 08:00. In the afternoon, Stefan Sommer presented first results of the cruise at the Ocean Science Center Mindelo (OSCM). After a successful cruise the scientific crew of M156 left RV METEOR at the 2nd of August 2019.

5 Preliminary Results

5.1. Physical oceanography and biogeochemical water column measurements

5.1.1 Hydrography from CTD measurements

(J. Hahn, G. Krahmann, R. Link, F. Dilmahamod, D. Rudloff, F. Bunsen, B. Domeyer, S. Sommer)

CTD system and calibration

During M156, a total number of 59 CTD profiles were collected in most cases to a depth of 1200m, 8 profiles were conducted deeper and to the ocean bottom and 16 profiles were conducted to a shallower depth. CTD Profile 006 was aborted during downcast (at 2000m) due to a defect of the winch cable. The positions of the casts are listed in detail in section 7. During the whole cruise the GEOMAR SBE6, a Seabird Electronics (SBE) 9plus underwater unit, was used. It was attached to the GEOMAR GO3 rosette frame. The SBE6 was equipped with one Digiquartz pressure sensor (s/n 1149) and double sensor packages for temperature (T), conductivity (C) and oxygen (O2) (primary set: T1 = s/n 2463, C1 = s/n 2443, O1 = s/n 1312; secondary set: T2 = s/n 2120, C2 = s/n 3959, O2 = s/n 1739). Additionally, a WET Labs fluorescence/turbidity sensor (ECO-AFL/FL, ECO-NTU, s/n 2294), a WET Labs CDOM fluorescence sensor (ECO CDOM s/n 2687) and a SPAR sensor (s/n 51) were attached to the SBE6. A PAR light sensor from Biospherical Instruments (s/n 4702) was attached to the SBE6 from CTD 041 onwards. All sensors worked well throughout the cruise. A Valeport altimeter (s/n 42299) was attached to the SBE6 to monitor the distance to the bottom, which worked out well. Data acquisition was done using Seabird Seasave software version 7.26.6.26. In order to collect water samples, 24 10-liter Niskin bottles were attached to the rosette frame. A SUNA sensor measuring nitrate concentrations (manufactured by Seabird Satlantic, s/n 345) was attached to the rosette frame during CTD 015 and 029-033. During some CTD profiles, several-minute-long stops were done during the upcast for calibration of external sensors (SUNA sensor, Seabird MicroCat, Aanderaa Optode).

For calibration of the CTD conductivity and oxygen sensors, water samples were taken from the Niskin bottles from almost every CTD profile. The samples were chosen such that they ultimately covered the whole range of the parameter (i.e. depth, temperature, conductivity, oxygen, time) space observed by all the CTD profiles. Conductivity values were determined from 253 water samples using an OPTIMARE Precision Salinometer (OPS) owned by GEOMAR and oxygen concentrations were determined from 297 water samples using Winkler titration (details are given further below).

CTD conductivity was calibrated using offset and linear dependencies of pressure, temperature and conductivity to match the salinometer derived values. CTD oxygen was calibrated using offset, linear dependencies of oxygen and pressure times oxygen as well as quadratic dependencies of pressure and temperature. The misfit, taken here as the root-mean square (rms) of the differences between CTD values and the respective water samples, was 0.00035089 S/m and 0.00034586 S/m for the C1 and C2 sensors, respectively. The conductivity misfit translates into a salinity misfit of 0.0034371 psu and 0.0034129 psu. The misfits for O1 and O2 sensors were 1.1372 and 1.119 µmol/kg, respectively. For each fit, the 33% most deviating water sample values were removed to exclude biases by bad samples. For the final data set that will also be publicly available, the primary sensor set was used for all CTD profiles. Data from the fluorescence and turbidity sensors and the PAR sensor was not calibrated against onboard reference samples, but with calibration coefficients provided by the manufacturer. No further corrections were applied. Data from the SUNA nitrate sensor was calibrated against 33 nitrate measurements taken from water samples during CTD profiles 015 and 029. The independently collected and processed nitrate data was later merged with the CTD data.

Conductivity measurements

Two GEOMAR OPS (serial numbers #10 and #20) were available onboard to analyze conductivity values from the water samples. However, we immediately found out that the stirrer of the pre-bath of OPS #20 was broken resulting in a non-stable pre-bath temperature. This OPS could not be used at all throughout the cruise and we only worked with OPS #10. The operation of an OPS has been tested for several years both in GEOMAR laboratories and on prior research cruises (see e.g. cruise report of RV METEOR M145) and we followed best practices as described in the following.

Flensburger bottles, which are well-established at GEOMAR, were used for taking water samples. Before measuring the respective conductivity with the OPS, the bottled water samples had to be degassed to remove gas micro-bubbles, which would deteriorate the OPS instrument performance. Degassing was prepared by warming the sample bottles in a water bath at a temperature of about 35°C-40°C. After one hour, the sample bottles were removed from the bath, they were immediately opened for a few seconds and then closed again. The sample bottles were brought to the OPS lab where their conductivity could be measured after 24 hours of equilibration to the lab temperature.

Throughout the cruise, the OPS was a couple of times standardized with IAPSO standard water. Substandard water samples were additionally used to directly identify drifts during measurement series of about 10 regular water samples. Substandard water samples are samples that were obtained by filling bottles with deep ocean water collected earlier and well-mixed in a 10 l water canister. At the beginning of the cruise, the stability and reproducibility of OPS measurements was checked with repeated measurements of substandard water samples. We observed downward drifts of the order of several 1/1000 psu in salinity during measurement of consecutive water samples, which we could relate to a too weak degassing of the sample bottles. Longer warming and a careful setting and keeping of the proper water bath temperature during the degassing procedure solved this problem. Non-visible micro-bubbles in the measurement cell of the OPS were removed by emptying the cell before starting the measurement series again. However, throughout the cruise,

we found an upward drift of several 1/1000 psu in salinity when comparing measurements of substandard water samples that were conducted before and after a measurement series of 10 regular water samples. This issue could not be observed during every measurement series and we could not identify the reason for this until the end of the cruise. For future cruises, we suggest to target this issue by frequently using IAPSO standard water, whenever a drift occurs.

During cruise M158 the same instrument (OPS #10) was on board and was inspected by the responsible technician (Boris Kisjeloff). He also found the measurements to be less stable than typical for the OPS salinometers. He discovered that one of the electronic boards had small traces of corrosion, most likely from a small leak in the internal tubing. On M158 the electronics board was exchanged with another one and subsequently the OPS measured reliably (see cruise reports for M158 and M159).

Oxygen measurements

Water samples for the Winkler titrations of dissolved oxygen were drawn from the Niskin bottles before all other water samples were taken to limit any distortion by outgassing of the water. The sample bottles (66 mL Wheaton bottles) were flushed at least three times by overflow to ensure air-bubble free samples. Oxygen fixation was carried out directly after sampling. 1 mL of each of the two fixation solutions (NaI/NaOH and $MnCl_2$) were dispensed with a high precision bottle-top dispenser (0.4-2.0 mL, Ceramus classic, Hirschmann). One dispenser broke during the cruise and from CTD 038 onwards, the fixation solution $MnCl_2$ needed to be added to the water sample by using a 1 ml hand pipette and later on by using a 1 ml syringe. The samples were stored in the dark prior to measurement.

Titrations with thiosulfate solution were performed within the Wheaton bottles using a 5 mL Burette Metrohm 876 Dosimat Plus Titration unit. Three thiosulfate solutions were subsequently prepared throughout the cruise. Standard measurements for the determination of the thiosulfate factor were carried out on a daily basis by adding an iodate standard with a 0.5-5 mL Eppendorf Research Pipette. Initially, for water sample titrations from CTD 001-009 (against thiosulfate solution #1), potassium iodate was used as iodate standard, whereas for water sample titrations from CTD 010-040 and 041-058 (against thiosulfate solution #2 and #3), respectively, two solutions of potassium hydrogen di-iodate were subsequently used. The stoichometric relation for all solutions was prepared in the lab prior to the cruise such that it nominally should have fulfilled a factor of 5 for determination of the thiosulfate solution. However, using the potassium iodate standard during the first 009 CTD profiles, the thiosulfate factor was unusually low at about 4.84-4.91. The iodate standard for CTD 010-040 and 041-058 was between about 5.01 to 5.04. No independent Wako standard was used as second reference during the cruise in order to disentangle the contributions of the two potential errors. However, the thiosulfate solution #1 was measured during two subsequent days with the potassium iodate standard (related to CTD 009) and with the potassium hydrogen diiodate standard (related to CTD 010) resulting in thiosulfate factors of 4.87 and 5.02, respectively. We concluded that the first iodate standard was more erroneous and we extrapolated the thiosulfate factor related to CTD 010 to the water sample titrations related to CTD 001-009.

The standard deviation of the oxygen concentration measurements determined by Winkler titration was 1.15 µmol L^{-1} based on 126 replicate measurements (116 duplicate or triplicate measurements throughout all CTD casts, and 10 quintuplicates for CTD 010). When discarding those 33% replicates with the highest standard deviation (i.e. discarding 43 of 126 replicates), the standard deviation was 0.41 µmol L^{-1}. Based on the repeated triplicate measurements, some Wheaton bottles were identified as systematic outliers likely due to inaccurate bottle volumes resulting in inaccurate bottle factors.

CTD system preliminary results

37 of the 59 CTD profiles were performed for the survey of the 18°W, 18.5°N cyclonic eddy (Fig. 3.2.2 and 3.2.3). A full meridional CTD section from the southern to the northern eddy boundary (18°15'N and 19°15'N) was conducted consisting of 10 CTD profiles with a horizontal distance of about 9 nm (Fig. 5.1.1.1, 5.13.1). The corresponding velocity section is shown in section 5.1.3 (Fig. 5.1.3.2). The eddy was found with a low oxygen core, where minimum oxygen concentrations were well below 20 µmol kg^{-1} between 20 and 50 m depth. Low salinity was found in the core (corresponding to more South Atlantic Central Water originating from off the Mauritanian coast), whereas the northern and southern eddy boundaries were observed well oxygenated (80-100 µmol kg^{-1}) and more saline (corresponding to more North Atlantic Central Water from the open ocean). Chlorophyll was enhanced at the meridional eddy boundaries in the upper 40 m suggesting more intensified primary production, with highest chlorophyll concentrations at the northern boundary. Correspondingly, turbidity was highest at the northern eddy boundary, but a secondary maximum was found above the eddy core, at a meridional position where lowest oxygen concentrations were observed.

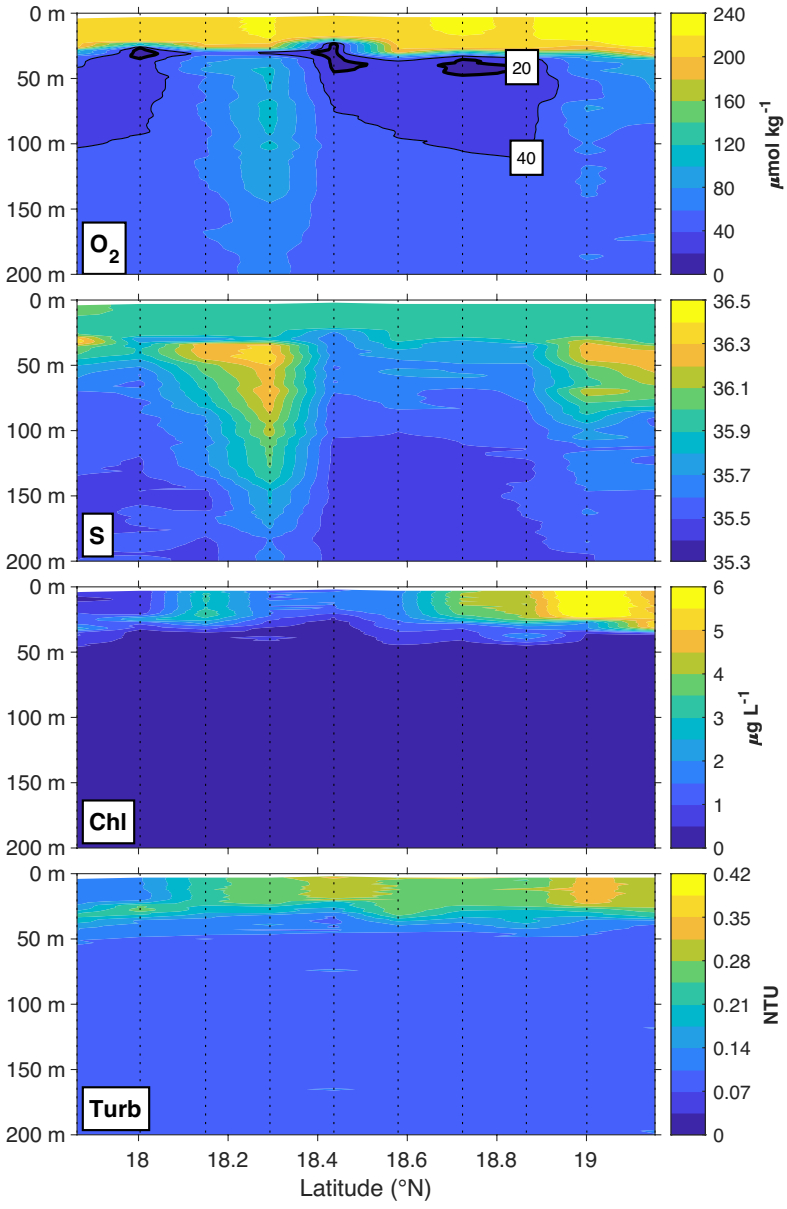

Fig. 5.1.1.1: Meridional CTD section along 18°05'W (section through the 18°W, 18.5°N cyclone) between 21-July-2019 and 24-July-2019. From top to bottom panel: dissolved oxygen, salinity, chlorophyll, turbidity. Positive values indicate eastward and northward velocity, respectively. Data is only shown for the upper 200 m (but available to a depth of 1200 m).

5.1.2 Turbulence measurements using microstructure sensors

(J. Hahn, F. Dilmahamod, R. Link)

A microstructure measurement program was carried out to quantify diapycnal mixing and associated diapycnal fluxes of oxygen, nutrients and other solutes in the open ocean. Primarily, the program aimed at advancing the understanding of the impact of mesoscale eddies on the diapycnal mixing processes. Mesoscale eddies change the stratification of the water column thereby impacting the temporal and spatial distribution of internal waves (Kunze et al. 1995; Karstensen et al. 2017). Further, they have an impact on the occurrence of submesoscale processes at horizontal temperature fronts primarily at the eddies' periphery, which may lead to locally enhanced diapycnal mixing (Klein and Lapeyre 2009; Brannigan 2016).

The measurement program consisted of shipboard microstructure sampling using a profiling system manufactured by Sea & Sun Technology. For these measurements, a MSS90-D profiler (S/N 73), a winch and a data interface were used. The loosely-tethered profiler was optimized to sink at a rate of 0.57 m s^{-1}. In total, 81 profiles were collected during 29 microstructure stations with a profiling depth between about 200 and 290 m, whereof 3 stations needed to be aborted without any profile due to a temporal defect of the winch. The profiles were always performed in the immediate vicinity of a CTD station, which has been conducted prior to or after the microstructure station. Most of the profiles were collected in the area of the 18°W, 18.5°N cyclonic eddy and some profiles were collected at the E stations (Fig. 3.2.2 and 3.2.3). The MSS profiler was equipped with three shear sensors, a fast-response temperature and oxygen sensor, an acceleration sensor, two tilt sensors and conductivity, temperature, depth sensors. During the whole cruise, shear sensor s/n 125 was attached to channel S1 (she1), shear senor s/n 135 was attached to S2 (she2) and shear sensor s/n 133 was attached to S3 (she3). When post processing the data, shear sensor s/n 125 was identified with a lower dissipation rate of turbulent kinetic energy compared to the other two shear sensors from profile 15 on. During the first 14 profiles, all three shear sensors consistently showed a similar dissipation rate. Very likely, this inconsistency from profile 15 onwards resulted from a reduced sensitivity of shear sensor s/n 125. The other two shear sensors s/n 135 and s/n 133 as well as all other sensors worked well throughout the whole cruise.

5.1.3 Vessel-mounted current measurements

(J. Hahn, F. Dilmahamod)

Technical aspects: Upper-ocean velocities along the cruise track were recorded continuously by the two vessel-mounted ADCP (vmADCP) systems of RV METEOR. The 38 kHz RDI Ocean Surveyor (OS38) system was operated in narrowband mode with 32 m bins and a blanking distance of 16 m while 55 bins were recorded. The 75 kHz RDI Ocean Surveyor (OS75) was operated in broadband mode recording 100 bins of 8 m length and a blanking distance of 4 m. The measurement range of the OS75 was about 600 m. The OS38 recorded valuable data to about 1400 m depth during the whole cruise. Data post-processing carried out for both systems included water track calibration of the misalignment angle and the amplitude of the Ocean Surveyor signal (Tab. 5.1.3.1). Note that prior to the cruise, the OS75 had been reported with one broken beam (beam #2), henceforth disconnected from the vmADCP deck unit. However, extensive cross checks of the OS75 velocity data (e.g. different data processing based on 3 beams vs 4 beams, comparison of backscatter data, consistency checks against velocity data OS38) were done during the cruise, but surprisingly no broken beam could be identified. All 4 beams were found without any unexpected mismatch and delivered data of reasonable quality.

Tab. 5.1.3.1: Misalignment angles and amplitude of the different Ocean Surveyors.

OS	Mode	Bin length	Misalignment angle ± standard deviation	Amplitude factor ± standard deviation
75	Broadband	8 m	-1.1282° ± 0.3843°	1.0033 ± 0.0095
38	Narrowband	32 m	0.0379° ± 0.5173°	1.0021 ± 0.0122

Preliminary results:

The vmADCP measurements allowed observations of upper-ocean velocities throughout the whole cruise. The main focus was on the survey of the 18°W, 18.5°N cyclonic eddy, whose position and extent was determined based on several vmADCP transects in combination with near real-time (NRT) satellite altimetry data. Geostrophic velocities from NRT satellite altimetry data were initially used to get a first rough estimate of the horizontal eddy core position as well as of the eddy shape (Fig. 5.1.3.1). A refined estimate of the core position was achieved by evaluating the most common intersection point of lines perpendicular to the observed shipboard velocities from the OS75 (assumption: geostrophic velocities). Satellite altimetry data suggested a slightly elliptic eddy shape, which has likely hampered a precise determination of the eddy core position. The core position was eventually estimated in the box 18°25'W - 18°05'W and 18°30'N – 18°45'N. Considering the meridional distance from maximum eastward to maximum westward swirl velocity, the eddy's extent was estimated between 18°15'N and 19°15'N (diameter of 1° or 60 nm). The eddy reached to a depth of several hundred meters (Fig. 5.1.3.2).

Two other eddies were crossed and observed with the vmADCPs during the cruise roughly at the following positions: an anticyclone at about 22°30'W, 19°30'N; an anticyclone off the Mauritanian coast at about 17°W, 18°N.

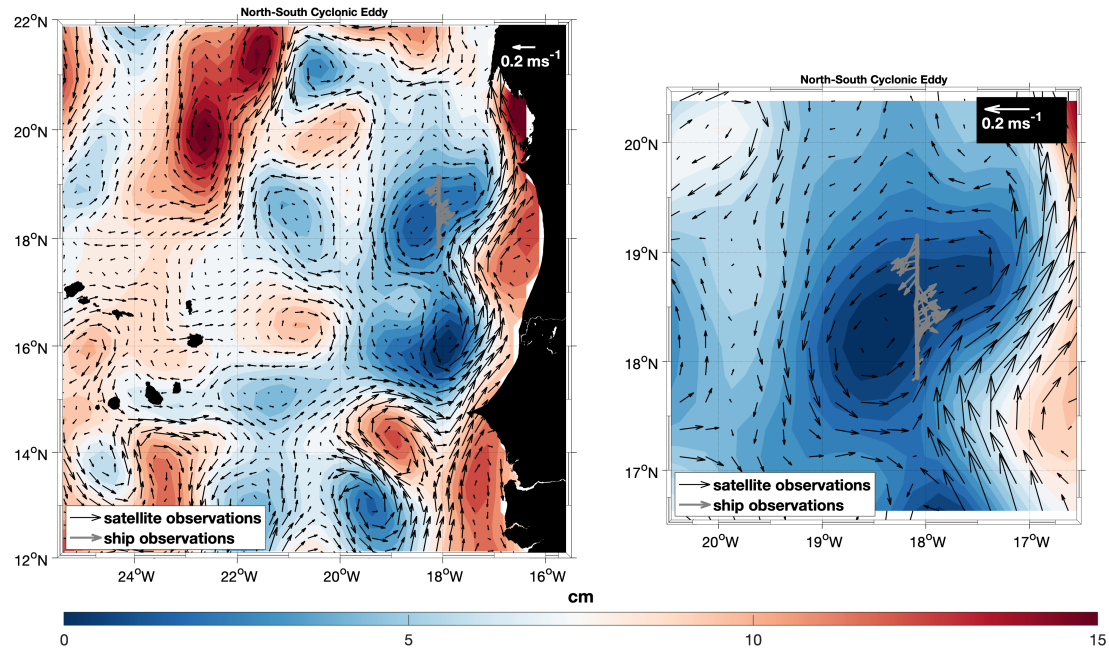

Fig. 5.1.3.1: Sea level anomaly (colored contours) and geostrophic velocities (black arrows) from near real-time satellite altimetry data from 22-Jul-2019. Gray line denotes ship track and gray arrows show depth averaged (50-300 m) velocities from the 75 kHz vessel-mounted Ocean Surveyor between 21-Jul-2019 and 22-Jul-2019. Right panel is a zoom of the left panel into the region of the 18°W, 18.5°N cyclonic eddy.

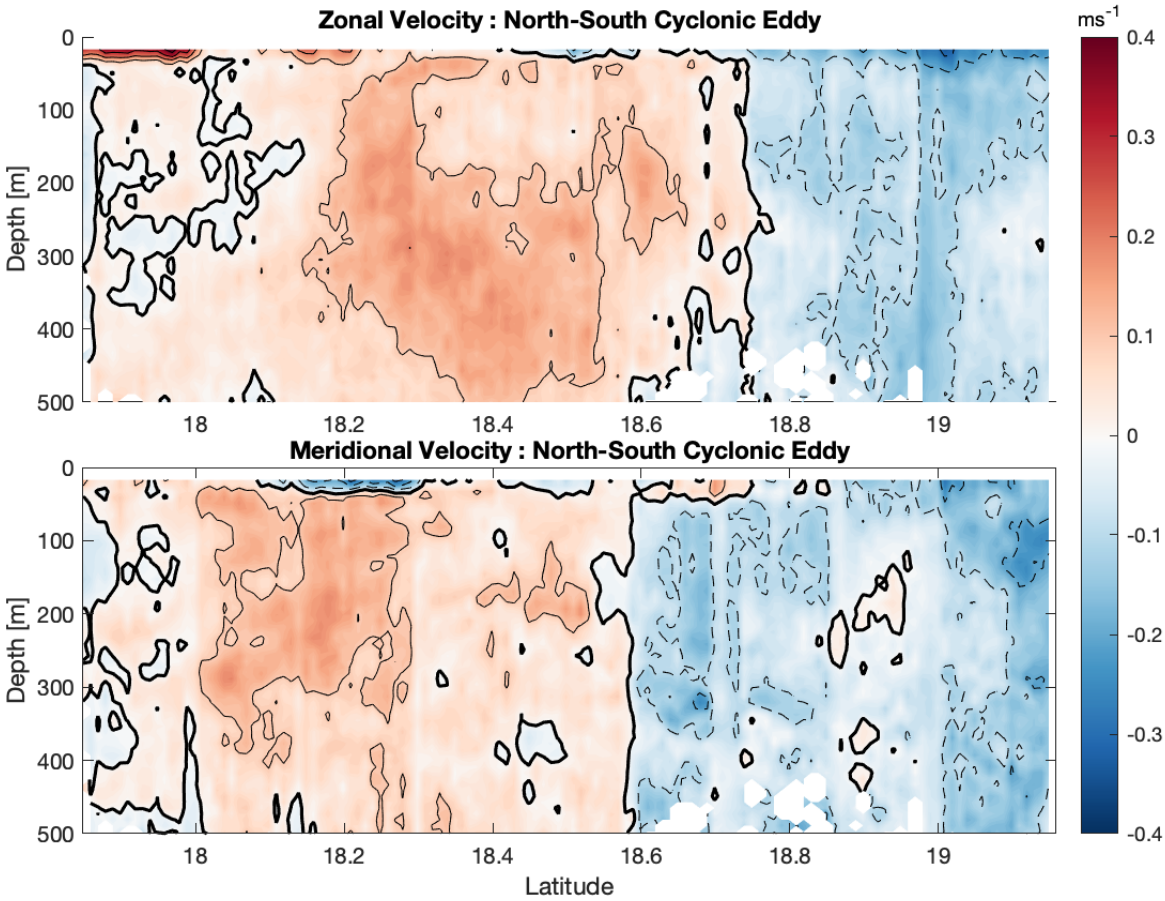

Fig. 5.1.3.2: (Upper panel) Zonal and (lower panel) meridional velocity along 18°05'W (section through the 18°W, 18.5°N cyclone) measured by the 75 kHz vessel-mounted Ocean Surveyor between 21-July-2019 and 22-July-2019 (ship track shown as gray line in Fig. 5.1.3.1). Positive values indicate eastward and northward velocity, respectively.

5.1.4 Glider operations

(J. Hahn, F. Dilmahamod, R. Link)

One Slocum glider owned by GEOMAR (ifm12) was used during the cruise to intensify the survey of the 18°W, 18.5°N cyclonic eddy. The glider was deployed on 24-Jul-2019 at 18°05'W, 18°35'N. It conducted an eastward transect along 18°42'N from the core to the periphery of the cyclonic eddy and was recovered on 28-Jul-2019 at 17°W, 18°42'N.

The glider was equipped with temperature, conductivity, pressure, chlorophyll (chl-*a*), turbidity and optode oxygen sensors. An optical nitrate sensor (SUNA, Satlantic) was mounted to the glider's top as a self-contained sensor package. The optical oxygen and optical nitrate sensor were in-situ calibrated by attaching them to the CTD rosette during a CTD profile. The optical oxygen sensor was additionally calibrated on-board in prepared water beakers against 0 and 100% oxygen saturated fresh water. During post processing, the conductivity sensor was identified with a changing response time throughout the deployment, which was noticed by a time varying delay between the conductivity and temperature time series. A probable reason could have been an inhomogeneous flow through the conductivity cell. However, this issue can be at least partly corrected by applying a time varying delay between conductivity and temperature. All other internal and external sensors of the glider worked well throughout the mission.

5.1.5 Water column nutrient, DIC and TA geochemistry in the 18.5°N, 18°W cyclonic eddy

(J. Hahn, M. Paulsen, E. Rickert, B. Domeyer, R. Surberg, S. Sommer)

During eddy generation, waters from the coastal upwelling region are trapped in its core and subsequently transported offshore. Hence, eddies can be considered as a continuation of the coastal upwelling system transporting solutes laterally into the open ocean. Thereby, they strongly modulate biogeochemistry, biological productivity and export production. It has been shown that the three different types of eddies (cyclonic, anticyclonic, anticyclonic mode water) have far-reaching effects. For example, in the upwelling region of northwestern Africa effects of eddies on subsurface oxygen concentrations leading to severe hypoxia and causing redox-dependent biogeochemical and biological responses, have been observed in a concerted field study (Fiedler et al. 2016, Hauss et al. 2016, Karstensen et al. 2015, 2017, Löscher et al. 2016). At the Cape Verde Ocean Observatory enhanced mass fluxes at about 3400 m water depth were observed during the passage of an anticyclonic mode water eddy (Fisher et al. 2016) likely affecting the otherwise oligotrophic deep-sea benthos.

During the detailed eddy study an intense nutrient geochemistry program was conducted along two meridional sections at 18°22'W (EDM stations) and at 18°5'W (EDM_E stations) as well as along a zonal section at 18°17'N, which during the time course of the cruise was shifted northwards to 18°34'N (EDZ stations) (Fig. 3.2.2 and 3.2.3). At the end of the cruise few stations were sampled along a zonal section at 18°N (AZM stations) across a suspected anticyclonic eddy. Though not further detailed here, further nutrient analyses were conducted at the main stations E1 to E5 including the side stations (S) and the Cape Blanc station CB (Fig. 3.2.2).

Water samples for nutrient analysis were obtained from 10 L Niskin bottles mounted to a CTD water sampling rosette (cf. section 5.1.1). In total 47 casts of the CTD water sampling rosette were analyzed indicated with "nutrients" in the station list, cf. section 7. The sampling of the Niskin bottles took place immediately after retrieval of the CTD after all other samples were taken. Subsequently the samples were stored in a fridge until further analysis. Within 24 hours after sampling, concentrations of nitrate (NO_3^-), nitrite (NO_2^-), phosphate (PO_4^{3-}) and dissolved silica were measured on-board using a QuAAtro autoanalyzer (Seal Analytical) with a precision of ±0.1 µmol L^{-1}, ±0.1 µmol L^{-1}, ±0.2 µmol L^{-1}, and ±0.24 µmol L^{-1} respectively. Ammonium was measured fluorometrically with the autoanalyzer using the ortho-phthalaldehyde (OPA) reagent.

As already outlined in section 5.1.1 the eddy core was characterized with low oxygen and low saline waters originating from the Mauritanian coast, which were characterized with elevated phosphate concentrations (Fig. 5.1.5.1). In contrast, the periphery of the cyclone was characterized by higher oxygen levels extending down to more than 200 m water depth. These higher oxygen levels coincided with low levels of nitrate and phosphate. Whether this is caused by eddy driven lateral water mass advection or downward mixing of surface waters awaits further analysis.

In addition, a total of 300 discrete samples for inorganic carbon parameters, e.g. DIC (dissolved inorganic carbon) and TA (total alkalinity), were taken in 250 ml glass bottles with glass stoppers, following the recommendations from (Dickson, Sabine & Christian, 2007). Sample analysis will be done in the home lab at GEOMAR, Kiel. DIC analysis will be carried out using a coulometric titration method using the SOMMA (single operator multi-parameter metabolic analyzer) system. Therefore, an accurately known volume of seawater will be dispensed into a stripping chamber and acidified. CO_2 is then sparged from the solution, dried and delivered to a coulometer cell.

Herein CO_2 reacts with the solution, building an acid that is titrated with in-situ produced OH^- ions. A semi-automatic analyzer, the VINDTA instrument (Versatile Instrument for the Determination of Titration Alkalinity), will be used to determine the Alkalinity. Therefore, seawater is titrated with a strong acid while following the EMF of a proton sensitive electrode. The resulting titration curve shows two inflection points, characterizing the protonation of carbonate and bicarbonate, respectively, with the acid consumption up to the second point equalling the titration alkalinity.

These measurements represent an important data base to interpret specifically the data described in section 5.1.6 and contribute to the overarching synthesis of all data obtained during the three REEBUS/MOSES cruises.

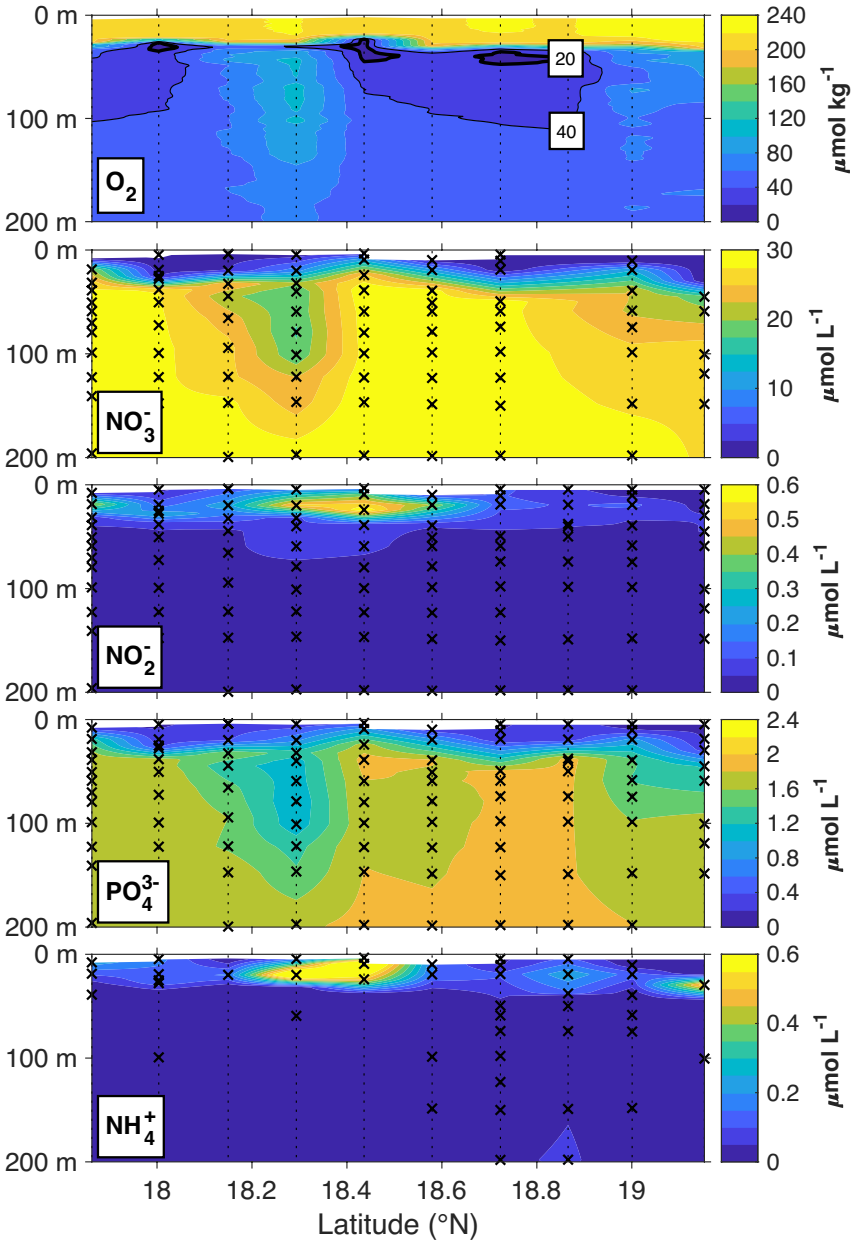

Fig. 5.1.5.1: Meridional distributions of oxygen (O_2), nitrate (NO_3^-), nitrite (NO_2^-), phosphate (PO_4^{3-}) and ammonium (NH_4^+) along 18°5' W through the 18°W, 18.5°N cyclone. The eddy center extends from ~ 18.4° to 18.9°.

5.1.6 CTD-rosette and marine snow catcher sampling for pelagic biogeochemistry

(K. Becker, Q. Devresse, T. Klüver, J. Roa and A. Engel)

Overview

Mesoscale eddies formed at Eastern Boundary Upwelling Systems (EBUS) are important vehicles for nutrients and carbon to the open oligotrophic ocean that influence the biogeochemistry on relatively small spatial scales (on the order of 100 km). They impact upper-ocean chemistry and biology through a number of processes. For example, in cyclonic eddies upward nutrient supply to the euphotic zone typically results in intensified primary productivity and changes in community structure, both of which affect export fluxes of carbon to the deep ocean. Therefore, the factors that control the (sub)mesoscale dynamics of the upper ocean are essential to understanding the efficiency of the biological carbon pump. However, the governing dynamical processes are largely unknown, and so is the overall biogeochemical and ecosystem response. To investigate the horizontal and vertical variability of organic matter and microbial activity within and around mesoscale eddies, we collected samples along a zonal corridor of the westward propagation of eddies between the Cape Verde Islands and Mauritania as well as from a cyclonic eddy at high spatial resolution. We particularly seek to understand the influence of (sub)mesoscale eddies formed in EBUS regions on (i) upper ocean organic carbon distribution, (ii) microbial productivity and organic matter turn-over and (iii) supply of organic matter to the central Atlantic Ocean. Our main objectives of the CTD-rosette sampling program were the detailed acquisition of upper ocean water column profiles. At 28 CTD stations (Fig. 5.1.6.1), water samples were collected from 7 depths for a variety of biogeochemical parameters including dissolved, non-sinking and other particulate organic matter components, microbial process rates as well as microbial cell abundances (Table 5.1.6.1). We collected a total of 185 samples (in replicates) for all DOM and POM parameters. For the microbial process rates, fewer samples were collected because of the more time-consuming sample processing, which includes incubations. All DOM and POM samples were shipped frozen or cooled to the home laboratory at GEOMAR and will be analyzed within the next year.

Dissolved organic matter sampling

Marine dissolved organic matter is the largest ocean reservoir of reduced carbon. It is predominantly produced autochthonously by photosynthetic plankton in the surface ocean, and it serves as substrate to vast heterotrophic microbial populations and as a source of nitrogen and phosphorus to nutrient-limited autotrophs (e.g., Azam et al., 1983). In order to describe the in-situ substrate availability for bacteria and archaea in and around mesoscale eddies, water samples for dissolved organic carbon (DOC), total dissolved nitrogen (TDN) and dissolved organic phosphorus (DOP) concentrations as well as concentrations and composition of dissolved amino acids (DAA) and dissolved carbohydrates (DCHO) were collected from all pelagic biogeochemistry CTD stations. Additionally, samples for chromophoric DOM (CDOM) and fluorescent DOM (FDOM) analysis were taken to assess their potential utility as tracers for eddy dynamics and vertical DOC fluxes. All samples were filtered on-board and stored at +4°C or -20°C, respectively. After shipment to the home laboratory, DOC will be analyzed with a high temperature combustion method after Sugimura and Suzuki (1988) and Engel and Galgani (2016). DOP will be analyzed after Grasshof et al. (1999). For analyses of DAA, the high-performance liquid chromatography method after Lindroth and Mopper (1979) will be applied. DCHO will be analyzed according to Engel and Händel (2011). CDOM will be estimated from spectral adsorption and FDOM from spectral fluorescence measurements and measurement will be compared with data from glider mounted ECO Triplet sensors (WETStar) to allow for extrapolation in space and time (Loginova et al., 2016).

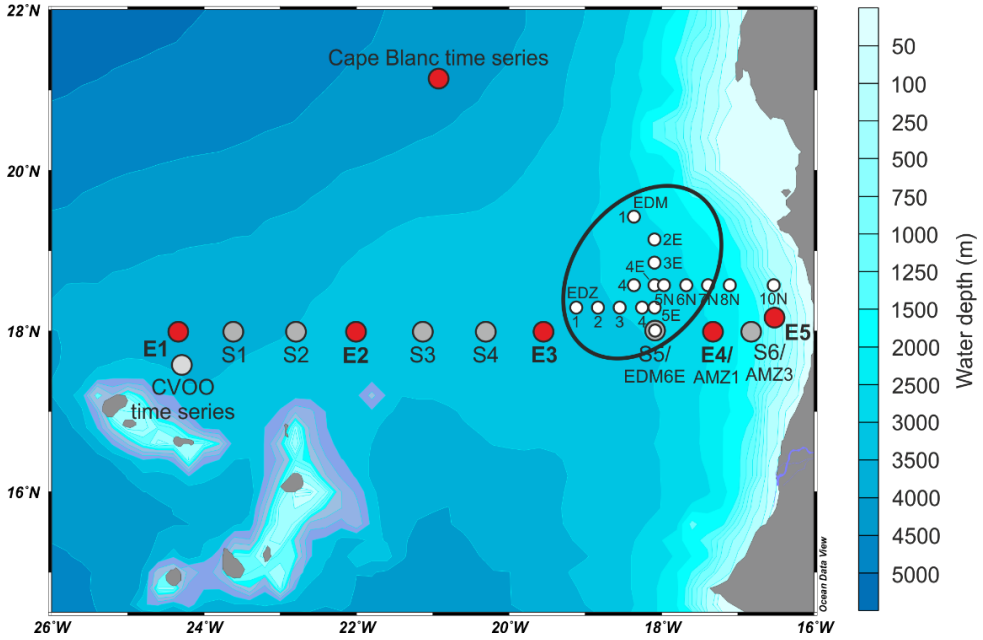

Fig. 5.1.6.1: CTD sampling locations for pelagic biogeochemistry. The black circle indicates the location of the eddy sampled at high spatial resolution.

Non-sinking organic matter sampling

Organic colloids and gel particles, i.e., polysaccharide-containing transparent exopolymer particles (TEP) and protein-containing Coomassie stainable particles (CSP), are an important component of the particulate organic carbon pool. They represent important microbial habitats and comprise significant fractions of extracellular organic carbon and nitrogen (e.g., Cisternas-Novoa et al., 2015; Busch et al., 2017). Since they are neutrally buoyant, they are transported with the water masses unless incorporated into sinking aggregates, which makes them interesting study objects for the investigation of carbon dynamics in eddies. TEP and CSP particles were sampled at all pelagic biogeochemistry CTD stations (see Fig. 5.1.6.1) following the procedures described in Alldredge et al. (1993) and Long and Azam (1996). Samples will be analyzed in the home laboratory following the method of Engel (2009).

Particulate organic matter sampling

Particulate organic matter (POM) in seawater plays a key role in oceanic carbon cycling and is composed of both living organisms and nonliving organic matter with the latter generally being its major component. Phytoplankton producers dominate the organic composition of POM in oceanic surface waters, and the plankton community structure generally modulates the recycling and export of organic materials in and out of the euphotic zone. It has for example been suggested that mesoscale eddies can have a profound impact on surface ocean POC fluxes (Omand et al., 2015). To investigate the particulate organic matter composition, we collected samples for total particulate organic carbon (POC) content as well as pigment and lipid compositions. The latter two analysis do not only provide information about the sources and fate of POM, but also about the adaption strategies of phytoplankton to their surrounding environment. All POM samples were collected in concert with the DOM and non-sinking organic matter samples, filtered onto GFF filters, flash-frozen (only the samples for lipids and pigments) and stored at -80 °C. Lipids and pigments will be analyzed according to Wörmer et al. (2013) and Becker et al. (2018). In order to analyse the abundance, distribution and community structure of pico- and nanophytoplankton as well as bacteria and viruses, we collected samples for flow cytometry analysis at GEOMAR.

Determination of microbial process rates

The influence of eddies on plankton-mediated carbon fluxes can further be assessed by measurements of primary and secondary production as well as aerobic microbial respiration rates. To determine primary production and release rates of organic carbon by phytoplankton, ^{14}C uptake measurements were conducted according to Nielsen (1952) and Gargas (1975). Microbial heterotrophic biomass production rates were determined using the ^{3}H-leucine incubation method (Kirchman et al., 1985; Smith and Azam, 1992). Bacterial respiration was determined during bioassays applying oxygen optodes following the protocol described in Vikström et al. (2019). With our results, we aim to contribute to a more comprehensive understanding on the functioning of eddies and their role in the biological carbon pump.

Table 5.1.6.1: CTD profiles and depths sampled for pelagic biogeochemical parameters.

Station	Lat (N)	Long (W)	Sampling depth (m) for DOM (DOC, DCHO, DAA, DOP, CDOM, FDOM)	Sampling depth (m) for POM (POC/N, Chl-a, Lipids, TEP, CSP, CLSM), bacterial biomass production, flow cytometry	Sampling depth (m) for primary production	Sampling depth (m) for microbial respiration
3 (E1)	17°59.996'	24°20.024'	5, 25, 75, 125, 200, 500, 800	5, 25, 75, 125, 200, 500, 800	5, 25, 75	5, 25, 75, 125
7 (S1)	17°59.966'	23°36.522'	5, 25, 75, 125, 200, 375, 800	5, 25, 75, 125, 200, 375, 800	-	-
11 (CVOO)	17°35.000'	24°17.000'	10, 20, 40, 60, 80, 100, 120, 150, 200, 250, 350, 450*	10, 20, 40, 60, 80, 100, 120, 150, 200**	-	-
13 (E2)	17°59.976'	21°59.969'	5, 25, 50, 100, 200, 450, 800	5, 25, 50, 100, 200, 450, 800	5, 25, 50	5, 25, 50, 100
21 (S2)	18°00.016'	22°47.077'	5, 25, 45, 100, 200, 390, 800	5, 25, 45, 100, 200, 390, 800	-	-
26 (S3)	17°60.000'	21°08.005'	5, 25, 50, 100, 200, 440, 800	5, 25, 50, 100, 200, 440, 800	5, 25, 50	5, 25, 50, 100
37 (Cape Blanc)	21°10.037'	20°54.983'	5, 25, 50, 95, 170, 460, 800	5, 25, 50, 95, 170, 460, 800	5, 25, 50	5, 25, 50, 95
43 (E3)	17°59.985'	19°33.005'	5, 25, 45, 90, 200, 400, 800	5, 25, 45, 90, 200, 400, 800	5, 25, 45	5, 25, 45, 90
50 (S4)	18°00.002'	20°18.012'	5, 25, 35, 100, 200, 485, 800	5, 25, 35, 100, 200, 485, 800	-	-
58 (EDZ1)	18°17.599'	19°06.790'	5, 27, 50, 100, 200, 400, 800	5, 27, 50, 100, 200, 400, 800	5, 27, 50	-
59 (EDZ2)	18°17.602'	18°49.571'	5, 15, 50, 100, 200, 400, 800	5, 15, 50, 100, 200, 400, 800	-	5, 15, 50, 100
66 (EDZ4)	18°17.543'	18°15.309'	5, 26, 35, 100, 175, 340, 800	5, 26, 35, 100, 175, 340, 800	-	-
70 (EDZ3)	18°17.574'	18°32.390'	5, 25, 33, 60, 150, 300, 800	5, 25, 33, 60, 150, 300, 800	-	-
75 (EDM1)	19°26.35'	18°22.206'	5, 22, 47, 86, 200, 350, 800	5, 22, 47, 86, 200, 350, 800	-	-
79 (EDM4)	18°34.771'	18°21.989'	5, 23, 40, 100, 200, 365, 800	5, 23, 40, 100, 200, 365, 800	5, 23, 40	5, 23, 40, 100
87 (EDM2E)	19°09.197'	18°05.18'	5, 30, 45, 100, 200, 400, 800	5, 30, 45, 100, 200, 400, 800	-	-
91 (EDM3E)	18°51.967'	18°04.981'	5, 20, 38, 50, 150, 300, 800	5, 20, 38, 50, 150, 300, 800	-	-
97 (EDM4E)	18°34.780'	18°04.954'	-	-	5, 33, 50	-
98 (EDM4E)	18°34.782'	18°04.953'	5, 15, 35, 60, 200, 400, 800	5, 15, 35, 60, 200, 400, 800	-	5, 15, 35, 60
107 (EDM6E)	17°59.818'	18°04.933'	5, 25, 32, 50, 200, 400, 800	5, 25, 32, 50, 200, 400, 800	-	-

113 (EDM5E)	18°17.603'	18°05.021'	5, 20, 32, 40, 100, 300, 800	5, 20, 32, 40, 100, 300, 800	5, 20, 32	-
125 (EDZ5N)	18°34.797'	17°57.999'	5, 20, 30, 100, 200, 350, 800	5, 20, 30, 100, 200, 350, 800	-	5, 20, 30, 100
130 (EDZ6N)	18°34.843'	17°40.788'	5, 14, 44, 100, 200, 300, 800	5, 14, 44, 100, 200, 300, 800	-	-
135 (EDZ7N)	18°34.793'	17°23.572'	5, 20, 40, 75, 170, 325, 800	5, 20, 40, 75, 170, 325, 800	-	5, 20
138 (E5)	18°09.960'	16°30.972'	5, 20, 52, 111, 150	5, 20, 52, 111, 150	5, 20, 52	-
143 (EDZ10 N)	18°34.943'	16°31.988'	10, 20, 44, 75, 119	10, 20, 44, 75, 119	-	-
151 (EDZ8N)	18°34.783'	17°06.358'	5, 17, 40, 125, 216, 375, 800	5, 17, 40, 125, 216, 375, 800	-	-
155 (AZM1)	17°59.994'	17°26.976'	5, 20, 31, 70, 118, 350, 800	5, 20, 31, 70, 118, 350, 800	-	5, 20, 31
158 (AZM3)	17°59.971'	16°55.393'	5, 28, 50, 130, 215, 400, 800	5, 28, 50, 130, 215, 400, 800	-	-
161 (E5)	18°10.244'	16°30.934'	-	-	-	5, 15, 35

***** only for DOC sampled
****** only for POC/N and Chl-a sample

Marine Snow Catcher sampling

Marine snow is an abundant and ubiquitous component of the marine water column, which affects the biology and chemistry of the ocean in multiple ways. For example, marine snow harbors concentrated microbial communities and contains unique chemical microenvironments where photosynthesis, decomposition, and nutrient regeneration occur at elevated levels compared to rates in the surrounding waters. During M156, marine snow samples were collected with the marine snow catcher (MSC), a ~100 L closing water bottle used to collect and settle sinking particulate material (Fig. 5.1.6.2a), at 15 stations from the surface mixed layer along the zonal transect and the cyclonic eddy (Table 5.1.6.2). At five of the 15 stations, the oxygen minimum zone, which was around 400 m for most stations, was sampled in addition to the surface mixed layer. Marine snow samples (see Fig. 5.1.6.2b and c for examples) were collected with a cut-off serological pipette from the bottom of the MSC after a settling period of 2 h for analysis of particulate organic carbon and nitrogen content (POC/N), particulate organic phosphorus (POP) particulate amino acid (PAA), particulate combined carbohydrates (PCHO), microbial lipid composition, transparent exopolymeric and coomassie-stainable particles (TEP and CSP, see Fig. 5.1.6.2d and e for examples of stained particles), and bacterial biomass production (BBP). Additionally, suspended POC samples were collected from the upper part of the snow catcher to compare measurements from the aggregates with the surrounding waters. Bulk aggregate and suspended samples were stored cooled or frozen and shipped to GEOMAR for analysis.

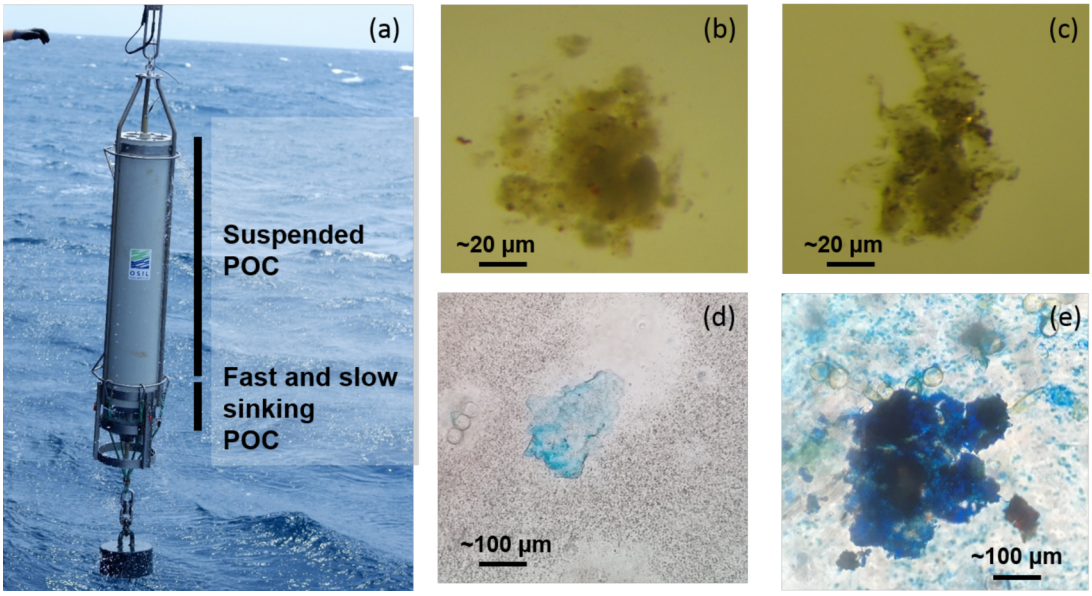

Fig. 5.1.6.2: a. Marine Snow Catcher (MSC), b. and c. examples of particles collected with the MSC, d. Aggregate from the MSC stained with Alcian Blue (staining of TEP material) and e. Aggregate from the MSC stained with Coomassie Brilliant Blue G (staining of CSP material; upper right).

Table 5.1.6.2: Station list for Marine Snow Catcher samples.

Station	depth (m)	Lat (N)	Long (W)	POC /N	POP	PCHO	PAA	Lip	CLSM	TEP	CSP	BBP
2 (E1)	20	18°00.005'	24°20.010'	x	x	x			x	x		
12 (E1)	500	17°59.996'	24°20.051'									
18 (E2)	450	18°00.001'	22°00.005'						x	x	x	
23 (E2)	25	17°59.998'	22°00.008'						x	x	x	
36 (Cape Blanc)	460	21°10.035'	20°54.982'	x	x	x	x	x	x	x	x	
45 (E3)	400	18°00.076'	19°32.933'	x	x	x	x	x	x	x	x	x
51 (E3)	25	17°59.982'	19°33.030'	x	x	x	x	x	x	x	x	x
57 (EDZ1)	25	18°17.596'	19°06.806'	x	x	x	x	x	x	x	x	
65 (EDZ4)	25	18°17.534'	18°15.345'	x	x	x	x	x	x	x	x	x
74 (EDM1)	25	19°26.325'	18°22.208'	x	x	x	x	x	x	x	x	x
80 (EDM4)	23	18°34.807'	18°21.988'	x	x	x	x	x	x	x	x	x
88 (EDM2E)	30	19°09.198'	18°05.021'	x	x	x	x	x	x	x	x	x
95 (EDM4E)	50	18°34.784'	18°04.996'	x	x	x	x	x	x	x	x	
99 (EDM4E	15	18°34.782'	18°04.953'	x	x	x	x	x	x	x	x	x
108 (EDM6E)	25	18°00.234'	18°04.965'	x	x	x	x	x	x	x	x	x
126 (EDZ5N)	350	18°34.796'	17°57.999'	x	x	x	x	x	x	x	x	x
139 (E5)	111	18°09.979'	16°30.984'	x	x	x	x	x	x	x	x	x
152 (EDZ8N)	17	18°34.793'	17°06.374'	x	x	x	x	x	x	x	x	x
156 (AZM1)	20	17°59.994'	17°26.976'	x	x	x	x	x	x	x	x	x
162 (E5)	20	18°10.246'	16°30.933'	x	x	x	x	x	x	x	x	

5.1.7 Waveglider and Lagrangian Drifter studies

(M. Paulsen, E. Rickert)

Submesoscale properties of the inorganic carbon system as well as the temporal and spatial variability of the net carbon uptake and oxygen utilization rates within eddys were the targets of our investigations. Therefore, a SV3 Wave Glider (Liquid Robotics, Sunnyvale, USA) equipped with a biogeochemical (BGC) sensor package was deployed July 14th 2019 at a station at 18°00.163'N, 19°32.766'W (water depth 3226m) and concluded its mission September 9th 2019 long after the M156 cruise ended. The recovery was carried out with the Cape Verdean Coast Guard vessel *Guardião*. During the deployment, the sensor package consisted of a pCO_2 sensor (HydroC®, CONTROS, Kiel, Germany, S/N CO2-1117-001), an oxygen optode (SBE63, Sea-Bird Electronics, Bellevue, USA, S/N 63-0392), a two-channel fluorometer (FLNTURT, Sea-Bird Electronics, Bellevue, USA, S/N 2493) measuring turbidity and fluorescence and a Mini TDGP (Pro-Oceanus Systems Inc., Halifax, Canada, S/N 38-511-31) to survey the total gas pressure of all dissolved gases. Furthermore, an ADCP (300 kHz Workhorse, RD Instruments, Poway, USA, S/N 1962) was for the first time installed to measure currents in the upper 100 m and test its usability as an eddy detection tool.

Two deployments of a lagrangian BGC drifter were conducted, one outside the eddy and one inside. The drifter was equipped with a sensor package similar to the Wave Glider consisting of a pCO_2 Sensor (HydroC®, CONTROS, Kiel, Germany, S/N CO2-0412-012), an Oxygen Optode (Aanderaa Instruments AS, Bergen, Norway, S/N 1082), a GTD pro sensor (Pro-Oceanus Systems Inc., Halifax, Canada, S/N 22-019-06) measuring the total gas pressure of all dissolved gases, a two-channel fluorometer (FLNTURT, Sea-Bird Scientific, Bellevue, USA, S/N 4897), a ProPS UV Photometer (TriOS, Oldenburg, Germany, S/N 028-05-D03E) and a CT sensor (SBE 37, Sea-Bird Scientific, Bellevue, USA, S/N 37IM60039). This sensor package was contained in a so-called sensor cage (Fig. 5.1.7.1) and attached to a spar buoy with a wire rope. Directly above the cage a drift anchor with a length of 6 m was placed to keep the sensors adrift within their water mass and not the surface current. The sensor package was deployed in two different depths outside the eddy at 100 m and inside at 35 m in the OMZ. Raw data of the second deployment can be seen in Fig. 5.1.7.2.

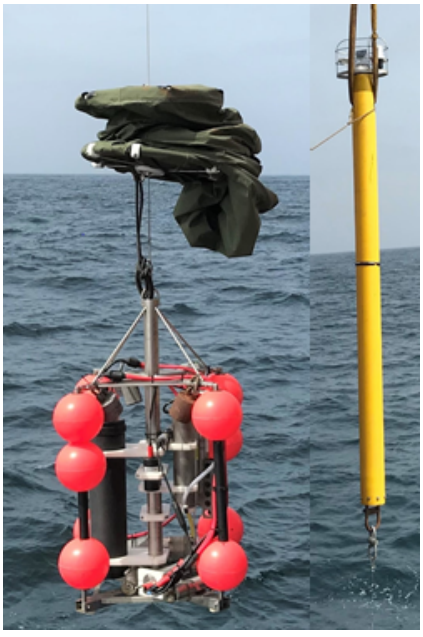

Fig. 5.1.7.1: Sensor cage with BGC sensors on top the folded drift anchor can be seen. Right: Spar buoy, which stays afloat and marks the drifter.

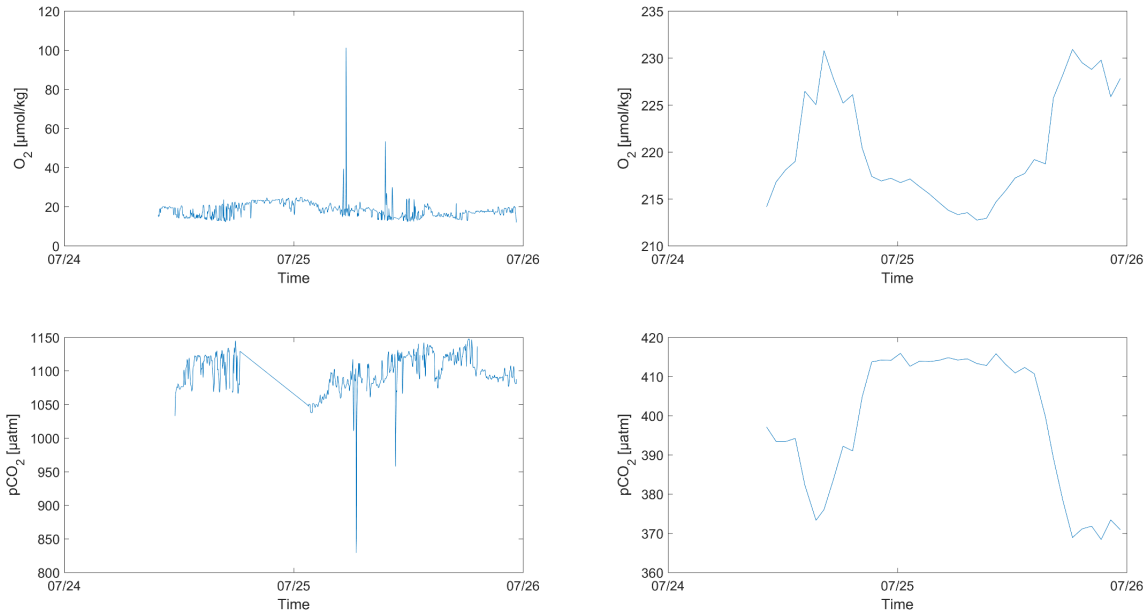

Fig. 5.1.7.2: Raw data for pCO_2 and dissolved oxygen. On the left data from the second drifter deployment is shown and on the right telemetry data from the Wave Glider which followed the drifter during its deployment.

5.1.8 Food web study in a cyclonic eddy

(S. Katzenmeier, H.-W. Breiner, T. Stoeck)

During the M156 cruise our goal was to analyse the protistan community structure across vertical gradients of an eddy and reference sites and to relate these structures to environmental variables. The second objective was to measure carbon fluxes mediated through protistan communities (top-down and bottom-up) and to model changes in the protistan community structure and function (carbon turnover) based on predictions of alterations in the EBUS.

Water samples were taken from the center of the eddy and its periphery as well as in between. At each station three different depths were collected from CTD casts. The deep chlorophyll maximum (DCM), the end of the photic zone (EPZ) and the oxygen minimum zone (OMZ) were selected based on measurements of auto-fluorescence and the oxygen concentration. For reference measurements, sites outside the eddy zone were investigated at the same depths.

DNA Analysis

The water samples were filtered on membranes immediately after sampling and conserved in a DNA stabilizing buffer until further processing in the laboratory. In the laboratory, the nucleic acids are extracted and purified according to our standard protocols. The genomic environmental DNA obtained is amplified with eukaryotic-specific primers (V9 region of the gene of the small ribosomal subunit) in a polymerase chain reaction (PCR). The obtained amplicons are sequenced using the Illumina HiSeq (NextSeq) platform (2x150 bp reads, paired-end).

The bioinformatic analysis of the obtained genetic data includes the assembly of the individual reads, the elimination of sequences of insufficient quality, the clustering of the sequence data at species equivalence level and the taxonomic assignment of the data. Statistical analyses include classical methods for comparative analysis of biocoenosis (alpha, beta, and gamma diversity), spatial analysis methods (TAR, mantle), ordination analyses, and graph theory-based network

analyses. In multivariate methods the obtained data of the protistan plankton community (PPC) are analysed together with the environmental parameters from other subprojects (especially WP1 and WP3). This allows a modelling (e.g. logistic regression models) of the dynamics of PPCs under the influence of environmental parameters caused by eddies and their space-time patterns.

Grazing Experiments

Water samples (1 l) taken from Niskin bottles were mixed with fluorescently labelled microspheres (10-15% of the concentration of the natural bacteria density in the sample). The samples were incubated under near in situ temperature conditions. At times of 0, 20, 45, and 90 min, subsamples were taken and immediately fixed using Lugol´s-formalin technique. The preserved samples were applied to Isopore membrane filters (millipore) for subsequent epifluorescence microscopy. After staining the filters with DAPI (4´,6-diamidin-2-phenylindole), the ingested food analogues in protists can be counted. The following information can be obtained from the data: The specific feeding rate (prokaryotes/protist/h), the grazing effect (prokaryotes/ml/h), and the turnover of the daily carbon biomass, each for the entire PPC and broken down by size fractions in the protistan plankton (picozooplankton, nanozooplankton, microzooplankton). Each approach was carried out in triplicates for statistical validation.

Observation of a red water bloom

At the 20th of July, an extended red tide was observed at the center of the cyclonic eddy (18°16.928'N 18°11.317'W), Fig. 5.1.8.1.

Fig. 5.1.8.1 **Left panel**, aerial view of the offshore red tide and the RV METEOR; **right panel**, detailed view of the red tide. (Image: H.-W. Breiner, TUKL).

Onboard microscopical investigations of a sea surface sample revealed that the tide is formed by ciliates of the species *Mesodinium rubrum* harboring the endosymbiotic cryptophyte *Teleaulax*. Whereas *M. rubrum* populations are common primary producers in many coastal and estuarine ecosystems, this bloom was observed offshore in about a distance of about 110 nm from the coast. Whether this bloom is due to fertilization caused by the deposition of Sahara dust or whether it is related to specific biogeochemical conditions created by the cylonic eddy can be only speculated.

Expected results

Through the assessment of the sequence data we obtain the protistan community structure across vertical gradients of eddies and reference sites and can relate these structures to environmental variables. The evaluation of the experiments will allow us to better understand the carbon fluxes

mediated through protistan communities. From the REEBUS project we expect the first information on the influence of possible changes in the CanCS on protistan plankton community structure and function (photosynthetic fixation and export of carbon from the surface ocean; transfer of bacterial carbon to higher trophic levels) as a cornerstone and marker for ecosystem functioning and stability/resilience.

5.2 Benthic biogeochmistry

5.2.1 Porewater geochemistry

(A. Dale, B. Domeyer, R. Surberg, T. Schmidt)

Objectives

The porewater composition of surface sediments was investigated at nine stations in order to characterize and quantify sediment diagenetic processes on the Cape Verde Terrace and eastwards to the oxygen-deficient waters offshore Mauritania. The main aim was to further our understanding of the carbon turnover through the eddy corridor. Specific emphasis was placed on the biogeochemical cycling and distribution of redox sensitive elements such as N, P and Fe and their relation to total oxygen uptake measurements measured in situ with the benthic landers.

Methods

An overview of the sampling stations where porewater geochemistry was analysed is given in Table 5.2.1.1 Sediment cores were retrieved using a multiple-corer (MUC). The MUC was equipped with 7 Perspex liners 60 cm long and with an internal diameter of 10 cm. The MUC was lowered into the sediment with a speed of 0.3 m/s in all deployments. Once on the seafloor, the liners were pushed into the sediment under gravity by a set of lead weights. Penetration did not exceed ca. 30 cm. Separate BIGO cores were taken by pushing the short liners (diameter 10 cm, length ca. 20 cm) into the sediment within the incubation chambers once the BIGO was back on deck. After retrieval, all cores were transferred to a cooling lab at 5°C and processed immediately; the bottom water temperature at the sampling stations was mainly ca. 2 ^{o}C, increasing to 15 ^{o}C on the Mauritanian shelf. Supernatant bottom water of the MUC cores was sampled and filtered for subsequent analyses. In general, one MUC and one BIGO sediment core was taken at the same site, but not necessarily on the same day. For all measurements and sub-sampling for redox-sensitive parameters (e.g. dissolved Fe, nutrients) from the MUC cores, the sediments were sectioned inside an argon filled glove bag. The sampling depth resolution increased from 1 cm at the surface to 4 cm at larger depths. Sediment samples were spun in a refrigerated centrifuge at 4000 G for 20 min at 3 ^{o}C to separate the porewater from the particulates. Subsequently, the porewater samples were filtered (0.2 µm cellulose-acetate syringe filters) under argon. All BIGO cores were processed in the same way but under ambient atmosphere. Porewater extraction yielded 5-30 ml of porewater at each depth interval. Sediment samples were also taken for the calculation of sediment density and water content as well as solid phase constituents in the onshore laboratory.

A total of 189 porewater samples were recovered and analyzed (Table 5.2.1.1). Porewater analyses of the following parameters were carried out onboard: ferrous iron (Fe^{2+}), nitrate (NO_3^-), nitrite (NO_2^-), ammonia (NH_4^+), phosphate (PO_4^{3-}), silicate (H_4SiO_4) and total alkalinity (TA). NO_3^-, NO_2^-, NH_4^+, PO_4^{3-}, and H_4SiO_4 were determined using standard methods (Grasshoff et al., 1997). NO_3^- and NO_2^- were measured on a Quaatro Autoanalyzer (Seal Analytic). NH_4^+ and PO_4^{3-}

were measured mainly on the autoanalyzer. At some stations, NH_4^+ and PO_4^{3-} were measured on a Hitachi U-2001 spectrophotometer (Table 5.2.1.1). The two instruments showed an agreement to within < 5 %. Porewater H_4SiO_4 was measured on the spectrophotometer. All samples from the BIGO syringes for nutrient analysis were determined using the autoanalyzer. For the analysis of dissolved Fe^{2+} concentrations, sub-samples of 1 ml were taken within the glove bag, immediately stabilized with ascorbic acid and analysed within 30 cm after complexation with 20 µl of Ferrozin. Samples for TA were analyzed by titration of 0.5-1 ml pore water according to Ivanenkov and Lyakhin (1978). Titration was ended when a stable pink colour appeared. During titration, the sample was degassed by continuously bubbling nitrogen to remove any generated CO_2 and H_2S. The acid was standardized using an IAPSO seawater solution. Analytical precision and detection limits of each method are given in Table 5.2.1.2.
Untreated samples were also stored refrigerated for onshore analysis of chloride, bromide, and sulphate by ion-chromatography. Acidified sub-samples (30 µl suprapure HNO_3^- + 3 ml sample) were prepared for analyses of major ions (K, Li, B, Mg, Ca, Sr, Mn, Br, and I) and trace elements by inductively coupled plasma optical emission spectroscopy (ICP-OES). Dissolved inorganic carbon (DIC) will be determined on selected sub-samples in the shore-based laboratory. Dissolved hydrogen sulfide (H_2S) was not measured in any of the cores due to the expected low rates of organic matter degradation in the deep-sea and the fact that previous studies on the shelf at St. E5 failed to detect H_2S in the porewater (Dale et al., 2014).

Table 5.2.1.1: Stations, porewater sampling method and number of sediment samples measured in multiple corers (MUC) and benthic lander cores (BIGO). Data are organized by sampling area / station.

Core ID [a]	Area / station	Water depth (m)	Date (2019)	Lat. (°N)	Long. (°W)	Core length (cm)	No. samples
004 MUC 1	E1	3694	04-Jul	18°00.000'	24°20.011'	23	13
006BIGO2-1 [b]	E1	3718	04-Jul	18°00.003'	24°20.011'	0	0
016 MUC 3	E2	3315	07-Jul	17°59.888'	22°00.003	31	15
019 BIGO 2-3 K2	E2	3312	07-Jul	17°59.999'	22°00.004'	9	8
030 BIGO 2-5 K2	Cape Blanc (CB)	4195	10-Jul	21°10.004'	22°55.004'	10	8
038 MUC 4	Cape Blanc (CB)	4186	12-Jul	21°10.007'	22°55.004'	31	14
040 MUC 5	E3	3228	13-Jul	18°00.002'	19°33.006'	30	14
041 BIGO 2-6 K2	E3	3226	13-Jul	18°00.001'	19°33.005'	11	9
062 MUC 6	E4, EDZ4	2833	18-Jul	18°16.911'	18°11.526'	34	16
063 BIGO 2-7 K2	E4, EDZ4	2833	18-Jul	18°16.908'	18°11.528'	19	12
103 BIGO 1-3 [c]	E4, EDZ4	2820	23-Jul	18°14.238'	18°09.447'	0	0
071 MUC 7	Northern Lander Station (NLS)	2877	19-Jul	19°19.756'	18°45.236'	34	16
072 BIGO 1-1 K1	Northern Lander Station (NLS)	2874	19-Jul	19°19.804'	18°45.208'	17	11
117 MUC 8	New Eddy Centre (EDM4E)	2717	24-Jul	18°34.800'	18°05.000'	34	15
122 BIGO 1-4 [c]	New Eddy Centre (EDM4E)	2715	25-Jul	18°34.742'	18°05.007'	0	0
120 MUC 9	Southern Lander Station (SLS)	2958	25-Jul	17°46.117'	18°03.184'	32	15

104 BIGO 2-8 K2 [d]	Southern Lander Station (SLS)	2943	23-Jul	17°46.198'	18°3.200'	17	9
140 MUC 10 [e]	E5	182	27-Jul	18°10.268'	16°31.027'	30	14
141 BIGO 2-9 [f]	E5	182	27-Jul	18°10.268'	16°31.027'	0	0

[a] K1, K2 denotes if sediments from chamber 1 or chamber 2 (respectively) were sampled using a push-core.
[b] No data. Deployment failed.
[c] Only TOU (total oxygen uptake) was determined in the benthic chambers.
[d] PO_4^{3-} was measured on the spectrophotometer in this core.
[e] NH_4^+ and PO_4^{3-} were measured on the spectrophotometer in this core.
[f] No data. Overlying water ran out on deck due to sandy sediment.

Table 5.2.1.2: Analytical methods of onboard geochemical analyses.

Parameter	Method	Detection limit	Analytical precision	Analytical Accuracy
NH_4^+	Photometer	1 µmol/l	5 %	-
PO_4^{3-}	Photometer	1 µmol/l	5 %	-
Fe^{2+}	Photometer	1 µmol/l	5 %	-
Alkalinity	Titration	0.05 meq/l	3 %	4 %
NO_3^-	Autoanalyzer	1 µmol/l	1 %	-
NO_2^-	Autoanalyzer	0.1 µmol/l	2 %	-
NH_4^+	Autoanalyzer	0.2 µmol/l	2 %	-
PO_4^{3-}	Autoanalyzer	0.05 µmol/l	2 %	-
SiO_4^{4-}	Autoanalyzer	1.7 µmol/l	2 %	-

Onboard results

Preliminary results focus on the sediment porewater distributions of dissolved NO_3^- and Fe^{2+}. In the deep-sea stations that lie far offshore from the African mainland (E1, E2, CB), NO_3^- concentrations increased from the surface sediment of 20 µM to ~40 µM due the nitrification or particulate organic nitrogen. The data suggest that the peak in NO_3^- coincides with the O_2 penetration depth of ca. 5 – 8 cm. Below this depth, NO_3^- diffused downwards indicating slow consumption by denitrification. The fact that NO_3^- remains at detectable levs down to 28 cm suggest that the sediments at these deep-water sites must be very unreactive and receive a low supply of liable organic matter. In these cores, the presence of NO_3^- and lack of Fe^{2+} shows that NO_3^- either inhibits the dissimilatory reduction of particulate iron oxides or that any Fe^{2+} produced in the nitrogenous sediments is immediately oxidized by NO_3^-back to particulate Fe^{III}.

Closer to the mainland (E3), an increase in the flux of organic matter reaching the seafloor presumably accounts for the dramatic reduction of nitrate penetration depth (NPD) to around 5 cm. A NO_3^- peak is still observable, indicating an O_2 penetration depth of only 1-2 cm. Below the depth where NO_3^- disappears, Fe^{2+} becomes detectable, reaching concentrations of around 20 µM. This feature continues heading up the slope. Stations E4, EDM4E, NLS and SLS all lie on roughly the same bathymetry (2700 – 2900 m) and all show shallow NPDs of 2 – 4 cm and a build-up of Fe^{2+} to around 30 µM. The vertical spatial separation of dissolved NO_3^- and Fe^{2+} in the porewater

strongly indicates that Fe^{2+} is rapidly oxidized by NO_3^-, potentially coupled to denitrification and the formation of iron (oxy)hydroxide mineral phases:

$$Fe^{2+} + 0.2\ NO_3^- + 1.8HCO_3^- + 0.6\ H_2O \rightarrow Fe(OH)_3 + 0.1\ N_2 + 1.8\ CO_2$$

Similar proposals have been made for anoxic deep-sea sediments and from studies in anoxic water columns (Dhakar and Burdige, 1996; Scholz et al., 2016).
At the shallowest station on the shelf (St. E5), NO_3^- barely penetrates the sediment (< 1 cm) due to the high input of labile organic matter (Dale et al., 2014). The surface sediments down to 15 cm are almost completely ferruginous. Below 15 cm, Fe^{2+} remained at the detection limit (ca. 1 µM). No H_2S was detectable below 15 cm. Previous work along a depth transect at the same latitude showed that H_2S only became present in the porewaters (in the short MUC cores) at water depths shallower than ca. 100 m (Dale et al., 2014).

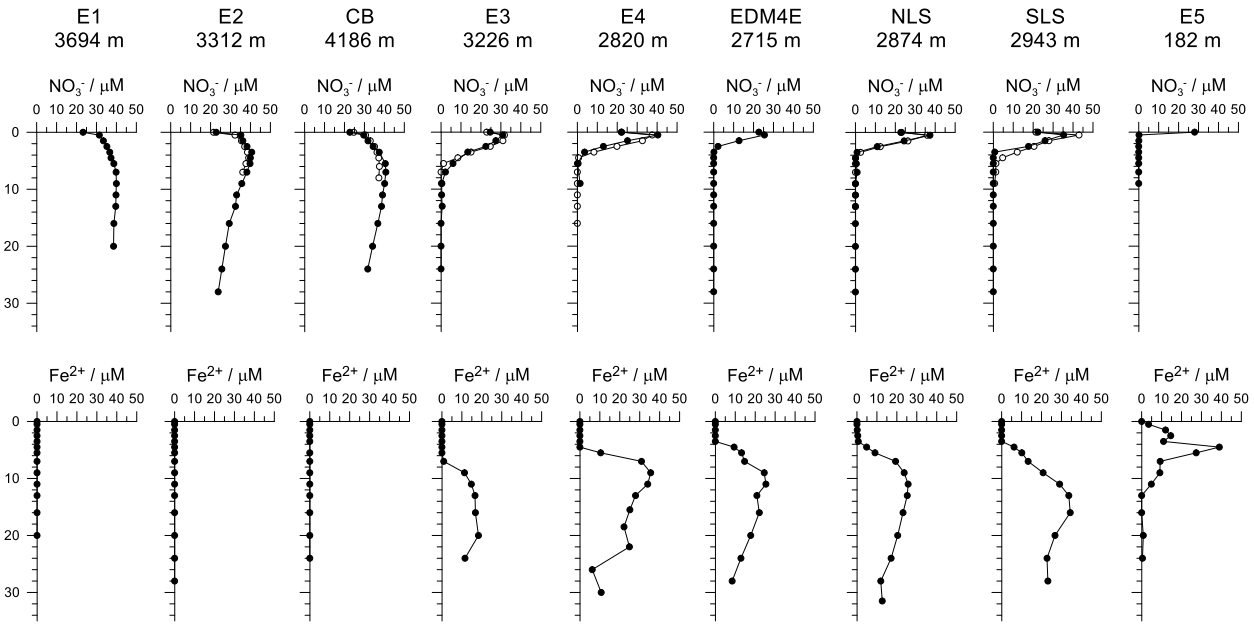

Fig. 5.2.1.1 Measured (symbols) concentration profiles of dissolved nitrate (top), dissolved ferrous iron (bottom) in sediments sampled by the multi-corer at all stations.

5.2.2 In situ oxygen and element fluxes

(S. Sommer, N. Bill, A. Dale, B. Domeyer, A. Petersen, T. Schmidt, T. Schott, R. Surberg, M. Türk)

The deep-ocean benthic community almost exclusively depends on allochthonous organic carbon, which is exported from the sea surface to the sea floor. By trapping coastal waters of upwelling origin and transporting them to the oligotrophic open ocean, eddies play an important role in the lateral mixing and transport of physical-biogeochemical properties and thereby modulate biological productivity and material fluxes to the seabed. Eddies have been shown to be important in the vertical export of organic matter (Fischer et al. 2016) and its transport to deep-sea sediments, thereby directly connecting surface ocean dynamics with the deep ocean (Zhang et al. 2014).

Major goal was to quantify the magnitude and variability of material turnover in the sediments underneath the eddy passage and to possibly link carbon turnover to eddy induced enhanced export production at the sea surface. In the typically oligotrophic deep-sea sediment organic carbon degradation is predominantly driven by using oxygen as the major electron acceptors. Hence major emphasis was placed on the measurement of total oxygen consumption.

In situ fluxes of primarily oxygen as well as silicate, total alkalinity, NO_3^-, NO_2^-, NH_4^+, and phosphate across the sediment water interface was determined to study carbon cycling and that of associated major elements in deep-sea sediments off Mauritania and Cape Verde.
Nine Lander deployments (BIGO, Biogeochemical Observatory) were conducted at the main stations E1 to E5 and off Cape Blanc as well as underneath a cyclonic eddy, Table 5.2.2.1, Figure 3.2.2 and 3.2.3. The eddy was identified based on satellite based altimetry data in conjunction with shipboard current measurements and when available by satellite based chl.a data.
Eddy sampling scheme: The investigations at the cyclonic eddy included three lander deployments at the supposed eddy center in water depths of 2715 to 2833 m, Figure 3.2.3. The bathymetry of the locations of BIGO-I-3 and BIGO-II-7 were investigated using the side-scan in addition to the shipboard multibeam system (cf. section 5.2.4). Both landers were deployed in a smooth terrain northwest of a small ridge structure. The lander deployment of BIGO-I-4 was conducted 21 nm to the north at a water depth of 2715. During the time course of the eddy investigation this position has been supposed as the new center of the cyclonic eddy. Further in-situ flux measurements were conducted at the northern eddy periphery 59 nm northwest of BIGO-I-4 in a water depth of 2874 m as well as at the southern periphery 48 nm to the south of BIGO-I-4 at a water depth of 2943 m. Care has been taken to conduct the lander investigation of the eddy at similar water depths. For time reasons the investigation of station E4 was omitted as the landers deployed in the eddy region were close by. During station work at the center of the cyclonic eddy at the 20. July an extended red tide, which was formed by ciliates of the species *Mesodinium rubrum* was observed. Whether the occurrence of the bloom can be linked to the specific biogeochemistry of eddy remains speculative.

Table 5.2.2.1: Station data of the in-situ flux measurements using the BIGO type lander.

Gear	Station	Date	Lat.	Long.	Depth (m)	Habitat
BIGO-II-1[a]	M156-6	04.07.19	18°00.003'N	24°20.010'W	3718	E1
BIGO-II-3	M156-19	07.07.19	17°59.999'N	22°00.004'W	3312	E2
BIGO-II-6	M156-41	13.07.19	18°00.001'N	19°33.006'W	3226	E3
[b]						E4
BIGO-II-9	M156-141	27.07.19	18°10.268'N	16°31.027'W	181	E5
BIGO-II-5	M156-30	10.07.19	21°10.005'N	21°10.004'W	4197	CB
BIGO-I-3	M156-103	23.07.19	18°14.238'N	18°09.447'W	2820	Eddy Centre
BIGO-I-4[c]	M156-122	25.07.19	18°34.742'N	18°05.007'W	2715	Eddy Centre
BIGO-II-7	M156-63	18.07.19	18°16.908'N	18°11.528'W	2833	Eddy Centre
BIGO-II-8	M156-104	23.07.19	17°46.198'N	18°03.200'W	2943	Eddy South
BIGO-I-1	M156-72	19.07.19	19°19.804'N	18°45.321'W	2874	Eddy North

[a] Deployment failed due to problems with the telemetry
[b] no lander deployment since this station was close to the southern periphery of the eddy
[c] new supposed eddy centre north to BIGO-I-3 and BIGO-II-7

For the measurement of solute fluxes across the sediment water interface and sediment retrieval two structurally similar BIGO´s (BIGO I and BIGO II) were deployed as described in detail by Sommer et al. (2009), Fig. 5.2.2.2.A. In brief, each BIGO contained two circular flux chambers (internal diameter 28.8 cm area 651.4 cm^2). A TV-guided launching system allowed smooth placement of the observatories at selected sites on the sea floor. Four hours after the observatories were placed on the sea floor the chambers were slowly driven into the sediment (~ 30 cm h^{-1}). During this initial time period where the bottom of the chambers was not closed by the sediment, the water inside the flux chamber was periodically replaced with ambient bottom water. The water body inside the chamber was replaced once more with ambient bottom water after the chamber has been driven into the sediment to flush out solutes that might have been released from the sediment during chamber insertion. To trace nitrogen fluxes, iron, phosphorous and silicate release as well as total alkalinity 8 sequential water samples were removed with a glass syringe (volume of each syringe ~ 47 ml) by means of glass syringe water samplers, Fig. 5.2.2.2B. The syringes were connected to the chamber using 1 m long Vygon tubes with a dead volume of 5.2 ml. Prior to deployment these tubes were filled with distilled water. Another 8 water samples were taken from inside of one of the two benthic chambers using an eight-channel peristaltic pump, which slowly filled glass tubes (quartz glass), Fig. 5.2.2.1B, C. These samples will be used for the gas analyses of N_2/Ar (Sommer et al. 2016) as well as DIC (Sommer et al. 2017). To monitor the ambient bottom water geochemistry an additional syringe water sampler and another series of eight glass tubes were used. The positions of the sampling ports were about 30 – 40 cm above the sediment water interface. O_2 was measured inside the chambers and in the ambient seawater using optodes (Aandera) that were calibrated before each lander deployment.

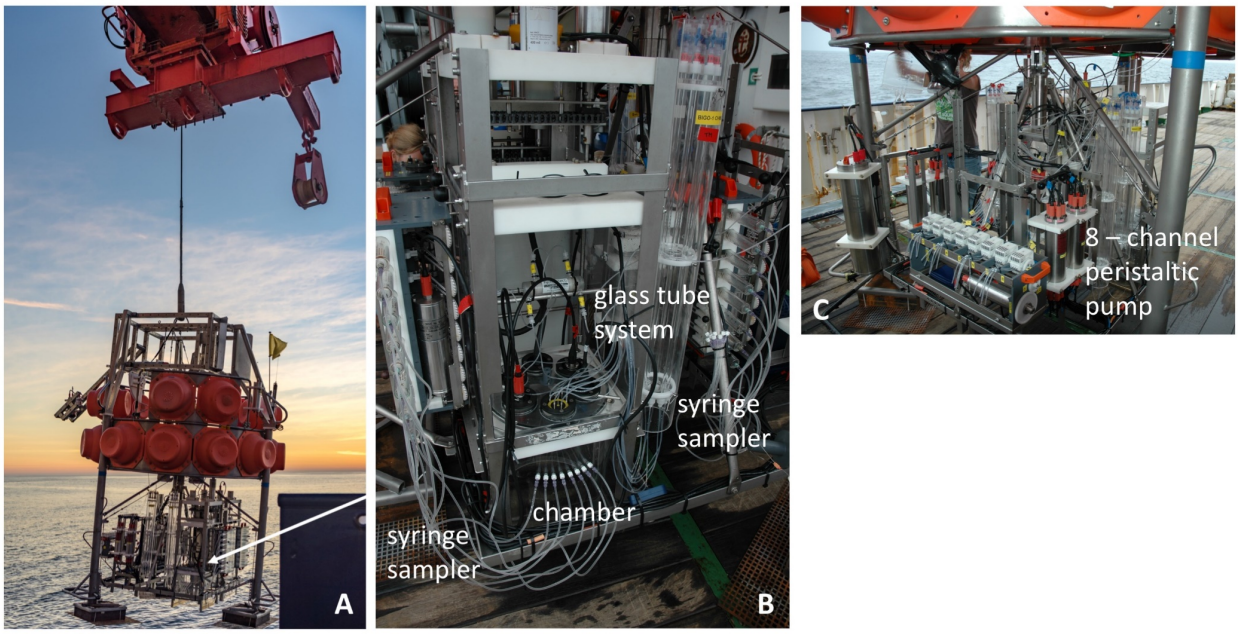

Fig. 5.2.2.2 **A** Lander and Launcher prior to deployment; **B** Flux chamber with attached syringe water sampler and the glass tube system; **C** 8-channel peristaltic pump for taking samples from the chamber and the ambient bottom water into the glass tubes (Image from Sommer et al. Cruise Report M137).

The in-situ O_2 flux measurements were complemented with ex-situ measurements of O_2 microprofiles that were performed in undisturbed sediments from the Multiple Corer. Microprofiles were measured at each station where the BIGO was deployed.

Onboard results

The oxygen raw data plotted versus time often displayed a non-linear decrease implying non-steady state particularly at the beginning of the incubation. In these cases, the oxygen fluxes were calculated using a polynomial curve fit of the oxygen raw data. Subsequently oxygen fluxes were calculated using the first derivative at the starting point of the experiment. Two examples of in situ oxygen chamber measurements are displayed for lander deployments underneath the suspected eddy center (BIGO-II-07) and at its southern periphery (BIGO-II-08), Figure 5.2.2.3.

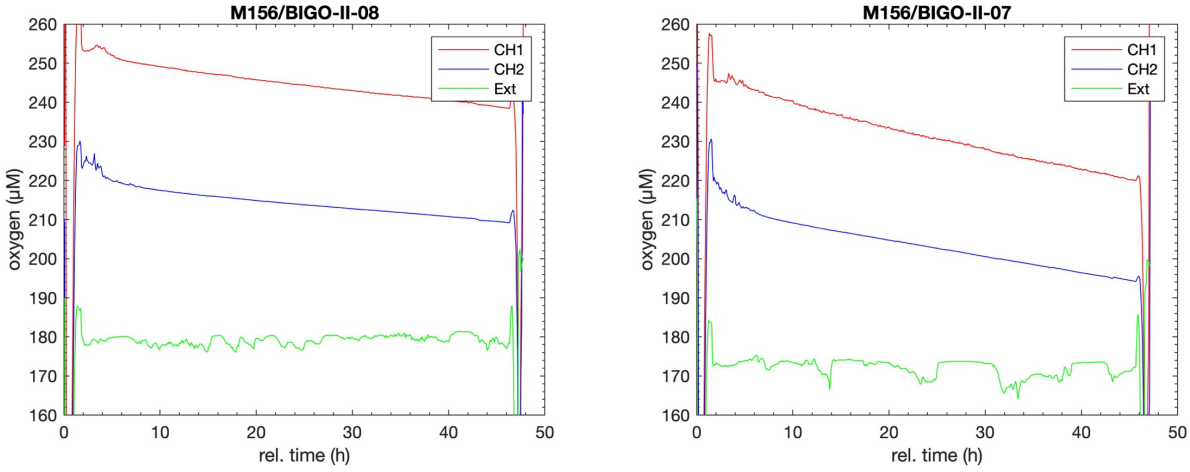

Fig. 5.2.2.3 In situ oxygen measurements (uncalibrated raw data) obtained from inside chamber 1 and 2 (CH1, CH2) and the ambient bottom water (Ext) underneath the suspected center (BIGO-II-07) of the investigated cyclonic eddy and its southern periphery (BIGO-II-08).

In total, 4 and 5 flux measurements were made under the periphery and the center of the eddy respectively. These flux measurements were conducted along a depth range of 2715 to 2943 m and display an enormous variability ranging from 0.96 and 6.51 mmol m^{-2} d^{-1} (preliminary data). The spatial variability is caused by the availability of organic carbon for respiration, which is governed by several factors including i. different depositional regimes of particulate organic carbon, related to surface water productivity affected by the passage of productive eddies, ii. the settling dynamics of organic particles and their biogeochemical alteration during their passage through the water column and iii. different accumulation of organic particles related to seafloor topography and bottom water hydrodynamics. All fluxes, except one where higher than the empirical equation relating total oxygen uptake to water depth provided by Wenzhöfer & Glud (2002) indicating a generally increased organic carbon availability in the investigated eddy area. The oxygen fluxes measured at station E2, E3, E5 and CB were similar to those estimated by the empirical equation. The oxygen flux at the shallow station E5 matched very well with previous measurements made in the same area during Maria S. Merian cruise MSM17/4 (Dale et al. 2014) and during METEOR cruise M107 (Sommer et al. 2015).

Expected results

The in-situ fluxes of primarily oxygen were measured in order to resolve the potential effects of enhanced carbon availability due to the passage of productive eddies for the deep-sea floor carbon cycling. In the investigated eddy area oxygen fluxes were generally rather high and indicate a trend towards higher oxygen fluxes in sediments underneath the eddy center compared to its periphery.

However, due to the limited data base of oxygen uptake rates (n = 9) we are not able to conclusively demonstrate that enhanced oxygen uptake underneath the eddy center is directly related to increased carbon input from the eddy, or merely reflects variability caused by factors such as for example different depositional regime of particulate organic carbon caused by seafloor topography and its interaction with the bottom water current regime. Despite these uncertainties, the obtained measurements strongly contribute to a better quantitative understanding of benthic carbon cycling processes in the largely under-sampled deep-sea.

We expect that at the 3rd research cruise within the REEBUS project, which presently is scheduled for October/November 2021, we will be able to better resolve the effects of eddy induced enhanced organic carbon supply by conducting a time series of oxygen fluxes using a mobile benthic Rover equipped with two benthic chambers. This Rover will be deployed for up to one year and recovered in 2022. This enable us to correlate time series of several parameters measured in situ at the deep-sea floor (imaging, fluorescence measurements, oxygen flux measurements, hydro-dynamical data) to eddy induced effects at the sea surface.

5.2.3 Microbiology of sediments underneath the eddy passage

(N. Adam, G. Schüssler, M. Perner)

In order to study the phylogenetic and metabolic diversity of benthic microorganisms along the zonal section at 18°N and to determine potential influences of eddies, sediment samples were taken by means of a video-guided multicorer device (TV-MUC). In total, 8 MUC stations along the 18°N transect and the eddy passage (E1, E2, E3, E5, Cape Blanc, “eddy center”, “south of the eddy” and a side station in a canyon structure) were sampled for microbiological analyses. Subsamples of the sediment cores were taken at 8°C in the following depths: 0-6 cm in steps of 1cm each, 6-14 cm in steps of 2 cm each, 14-30 cm in steps of 4 cm each and 30-35 cm (5 cm step). For each subsample 5 mL of sediment were frozen at -80°C for later RNA/DNA extractions and sequencing in the home lab and 0.5 mL of sediment were fixed with formaldehyde according to standard protocols for later cell counting (in the home lab). Additionally, for three stations (“eddy center”, “south of the eddy” and station E5), incubation experiments with sediment samples were performed. Sediment slurries were set up with artificial sea water and supplemented with defined amounts of different electron donors (i.e. H_2S, H_2 and Fe^{2+}). The consumption of the respective electron donors was monitored by measuring their concentrations in the slurries. Furthermore, incubations were set up with ^{14}C-labeled bicarbonate to monitor autotrophic CO_2-fixation. The data evaluation and calculation of electron donor consumption and CO_2-fixation rates will be done in the home lab, after counting of microbial cells in the sediment slurries.

In addition, enrichment cultures were set up with sediment subsamples of all sampled stations, offering different energy sources for microbial growth like H_2 and H_2S (Fig. 5.2.3.1). These enrichments will be continued and evaluated in the home lab.

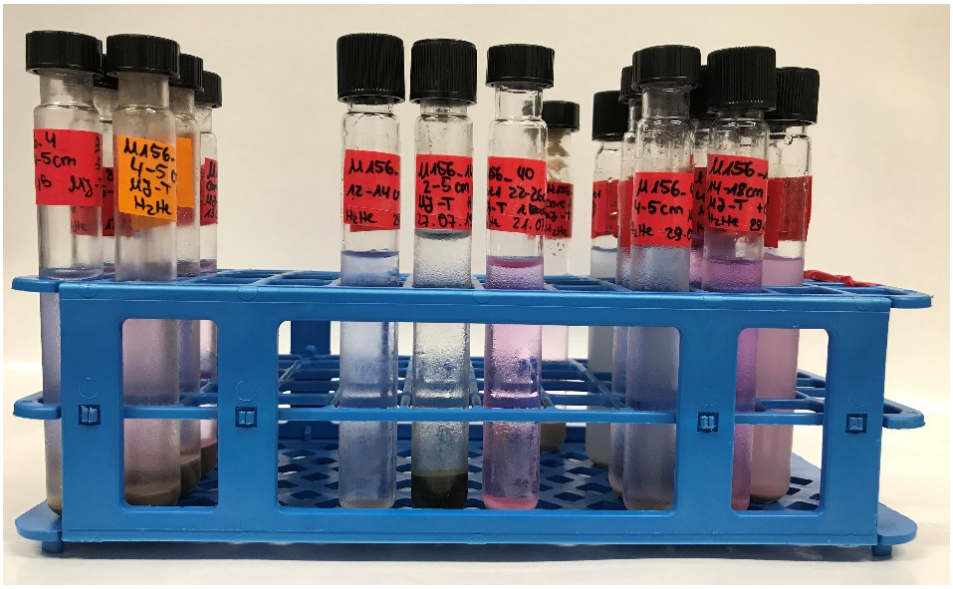

Fig. 5.2.3.1: Enrichment cultures containing artificial seawater medium, sediment samples and different substrates for microbial growth. Different colors of the media refer to different oxidation states and serve as an indicator of microbial activity.

For reasons of comparison, water column samples were taken by means of a CTD rosette (equipped with 10 L Niskin bottles) at 7 of the 8 microbiological sampling stations. For each water column sample 1 L of water was collected from the Niskin bottles, 10 mL of the sample were fixed with formaldehyde according to standard protocols for later cell counting. The rest of the water sample was drawn onto 0.22 µm filters to collect bacterial cells for later DNA/RNA analyses in the home lab. Filters were frozen at -80°C.

Expected results:
After conducting additional experiments in the home lab (i. e. counting of microbial cells as well as analyses of the benthic microbial metagenomes) and the evaluation of the obtained data, we expect to gain insights into the diversity and spatial distribution patterns of sediment-associated microbial communities along the 18°N transect and the eddy sites. By correlating the benthic microbial communities with the respective porewater geochemistry and the data from our incubation experiments, we will hopefully be able to identify key-drivers of microbially mediated element-cycling. Furthermore, these data (compared to those of the water column reference samples) will allow to determine potential influences of an eddy passage on the compositions and metabolic diversity of microbial communities of deep-sea sediments.

Data availability:
The digital sequence information obtained for the sediment samples taken during cruise M156 will be deposited in the GenBank database of the National Center for Biotechnology Information (NCBI). It will be made publicly available for research purposes upon publication of the results of the study.

Data type: digital sequence information; Contact person: Prof. Dr. Mirjam Perner, GEOMAR, mperner@geomar.de

5.2.4 Seafloor imaging, bathymetry, sidescan

(M. Kampmeier, M. Schuhmacher, T. Schott)

Eddy-induced downward carbon flux causes high spatial and temporal heterogeneity of benthic carbon turnover, which is superimposed by the variability induced by bathymetry, small scale seafloor morphology interacting with currents on the deposition of particles. This creates small scale variations that need to be considered when extrapolating from single point flux measurements to regional benthic element cycling. Detailed optical and hydro-acoustic studies are necessary to map sedimentological and depositional variations in such a detail that statistically valid and causal links can be drawn between seafloor morphology, sedimentological properties and biogeochemical fluxes.
Specific aims were to i. image and map the seafloor on different spatial scales to detect variations in seafloor topography and properties likely affecting the accumulation of particles at the seafloor; ii. to provide a sound background database to seek for possible correlations between seafloor properties and topography and geochemical measurements for spatial flux extrapolation; iii. to provide guidance for lander placements during the cruise.

Methods:
Multibeam Echosounder
Since multibeam echosounders (MBES) are a state-of-the-art tool for spatial seafloor mapping, RV METEOR is equipped with two hull-mounted Kongsberg MBES: EM 710 (70-100 kHz) and EM 122 (12 kHz). Their depth range depends on the frequency, whereby the EM 710 can reach up to 2,000 m and the EM 122 up to 11,000 m water depth. The EM 710 was only used on the shelf in shallow water.

Table 5.2.4.1: MBES settings

	EM 122	EM 710
Frequency	12 kHz	70-100 kHz
Beam opening angle	1° x 2°	1° x 1°
Swath	100°	100°
Survey speed	8 kn	8 kn
Filter	Spike filter: off, Tilt angle: 5°	Spike filter: off, Tilt angle: 5°
Beam spacing	Equi-distant	Equi-distant

Sound velocity profiles were applied for each area. The MBES was controlled and data were recorded with the system software SIS in *.all format. Post-processing was done with Qimera and FMGT (QPS). MBES profiles were planned to cover as much area as possible. Because most areas were very plain and noise inside the outer beams tends to overlay the morphology, the swath was chosen rather small (100°) and the overlap high (ca 50%). During post- processing, the refraction corrections were applied and the data cleaned from spikes and false detections. Data were then exported as ascii grid files and geotiffs. Additional to bathymetry, the MBES also records backscatter data of the seafloor. Depending on sediment roughness (mainly correlated to grainsize), the emitted sound is scattered back differently. Whereby soft and water saturated sediments generate low backscatter amplitudes (dB), harder or coarser material are characterized by high dB values. The backscatter is stored inside the *.all files and slope correction is done by merging it inside the software FMGT (QPS) with the processed bathymetry. Resulting backscatter grids were exported as ascii grid files and geotiffs.

OFOS

The Ocean Floor Observation System (OFOS) is a towed sledge that can carry multiple instruments to observe the sea bed. It is connected to an on-board computer system via cable and a telemetry and most commonly used to get a live view video footage of the seafloor.

During M156, nine OFOS surveys were undertaken. The areas have been selected according to their sediment properties and prior measurements. For each deployment, a high-resolution video system in combination with a CTD was installed on the OFOS frame. The ADCP was mounted once for down- & upcast to measure current velocity and direction in the water column. Also, an Ocean Imaging Camera (OIC) has been mounted on the sledge for a test run.

The OFOS was towed via a cable over the starboard side of the vessel at a speed of roughly 1.5 kn. Its final flying altitude over ground was attempted to be around 1.5-3m, depending on the swell. Three lasers arranged in an isosceles triangle indicated the forward-looking direction.

In the following section, the setting of the main instruments used with OFOS will be described briefly. The settings of OIC and ADCP can also be found in the BBL lander section as this was the major field of their application.

Sensors and settings**:**

Video Camera:

The video footage was taken with a 1.8 MP Canon Legria HFG10 at a shutter speed of 1/50 with focal length 35mm. During the first three surveys, the video recording was done via a frame grabber as the internal recorder of the camera was broken. However, this could be fixed and from the fourth survey onwards, high definition videos were recorded.

CTD:

To measure sea water physical properties, a CTD by RBR was used. It measured oxygen (optode), temperature, pressure, conductivity and turbidity at a sample rate of 10s.

ADCP:

The main settings are described in the BBL lander section. On the OFOS, the ADCP was mounted in a way that the beam 3 was rotated -45° in forward looking direction with the lasers taken as a reference.

OIC:

Due to dimension issues, the OIC was mounted instead of the video camera to test its operability and camera settings. The image sampling rate was set to one minute. For further settings please see section ‘BBL lander’.

The videos were sliced and converted to .jpg images every 20 seconds using ffmpeg. Subsequently, they were georeferenced and converted to geotiffs using the recalculated navigation and estimated heading from the videos with a custom script-based software and GDAL for raster geospatial data processing. An overview of the results can be seen on the map below (Fig. 5.2.4.1). A selection of geotiffs is superimposed to an OFOS track (coloured dots, Fig. 5.2.4.1 insert).

A major problem was encountered with the USBL navigation system Posidonia, which was planned to be used to obtain the correct position of the OFOS on the seafloor. Due to interference with the vessel-mounted ADCP, the measured positions deviated strongly and could not be accepted. Thus, during post processing, the positions were recalculated using the ship position from GNSS along with the measured cable length and ship heading. For future Posidonia-deployments, the vessel’s ADCP should be switched off.

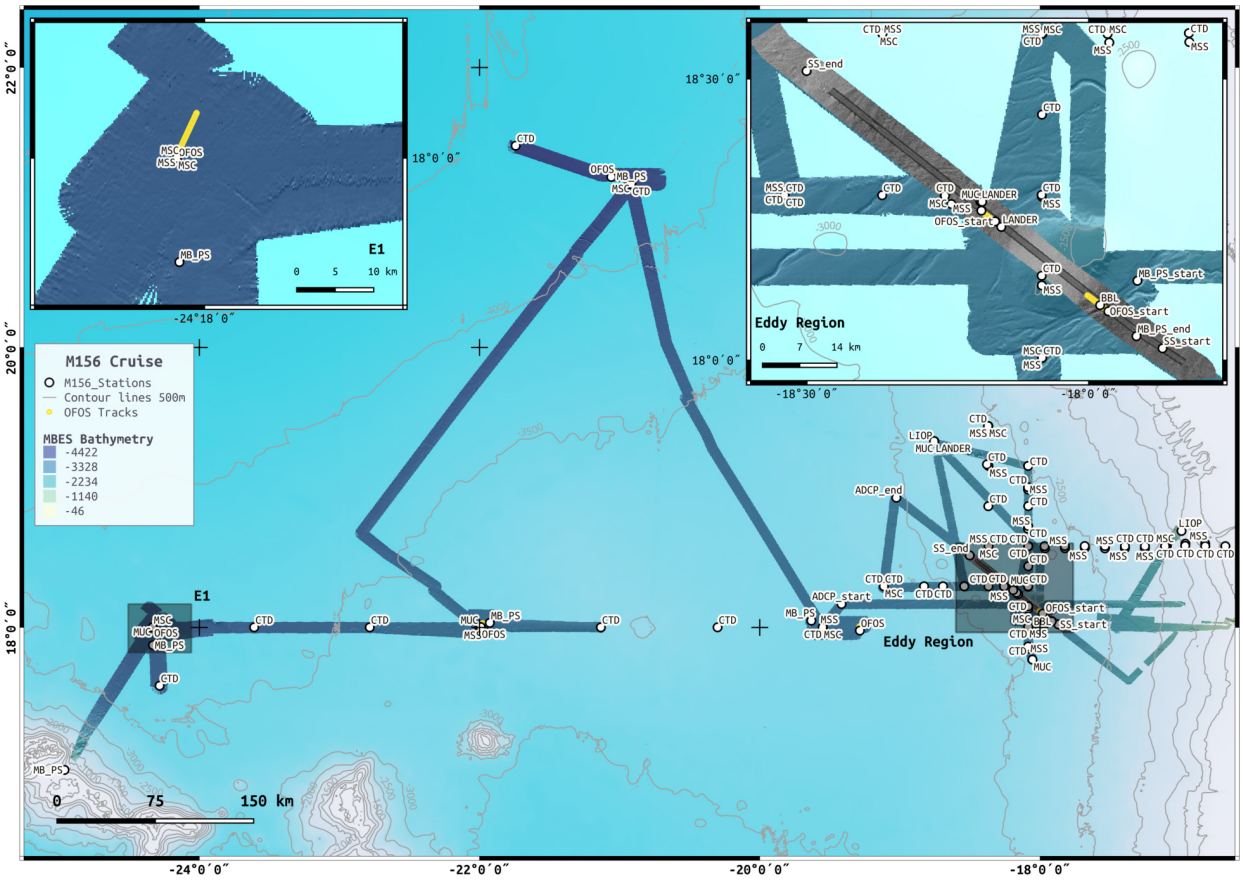

Fig. 5.2.4.1: Overview map of M156. The insert map shows the eddy region with the sea hill and canyons clearly visible. The yellow dots indicate OFOS tracks.

Sidescan Sonar

The GEOMAR-owned deep towed sidescan sonar (DTS) was used to acquire high resolution backscatter information from the seafloor. The system is towed behind the vessel using the 18 mm wire over the A-frame. A depressor decouples the tow-fish from ship motion and keeps it stable. Survey speed was limited to 1.5 - 3.0 knots. One 24-hours profile across a subsea hill within the Eddy Region was conducted. The DTS was operated with a frequency of 79 kHz and sub-bottom profiler (SBP) data were recorded at the same time and stored inside the sidescan file. Recorded *.JSF files were converted into *.XTF files and processed with the software CARAIBES by Ifremer. Layback was corrected via the cable length and a backscatter map was exported as geotiff.

BBL Lander

The BBL lander was deployed for 7.5 days south of the subsea hill inside a channel at a water depth of 3125 m (Fig. 3.2.3). A KUM sediment trap was installed in the center of the lander and equipped with two sampling bottles. The trap was programmed to turn the first bottle under the funnel four hours after the Lander was placed the sea floor. Unfortunately, the rotating mechanism to place the second bottle under the funnel mouth failed. Therefore, only one bottle was used to collect sinking particles, but could not be closed during retrieving the lander. Therefore, the sample does not only represent the sediment particles reaching the bottom, but also particles collected in the water column during lander retrieval.

The 300 kHz ADCP was installed facing upward on the topside of the lander. A sampling interval of one hour, and an opening angle of 20° and 30 sampling bins have been chosen.

Table 5.2.4.2: Sensors installed on the BBL lander with its specific data types and settings.

Sensor	Data type	settings
Ocean Imaging camera: Most of the settings despite the focus can be done via remote control using the Camera Control Pro software. To set the focus, the camera housing has to be opened to manually rotate the lens to the correct focus position. All settings were made for deep sea conditions (~ clear water):	Still photos	• Shutter speed: 1/60s • F-stop: 9 • Illumination: +1/3 • ISO: 400 • White Balance: Flash • Image quality: fine (fine + raw (.NEFF) if uncertain about outcome) • Focus: 1.5m @ 2m range (only manually, requires opening camera housing) • Photo interval: 10 min
ADCP	Water currents	300 kHz; Ping interval: 1 h
CTD	Conductivity Temperature	
Sediment trap	Marine snow	Only one bottle was filled

The sampling bottles were prepared as follows: The Bottles were filled to 1/3 with filtered seawater from lander depth. Subsequently, a formaldehyde-brine (980 ml filtered seawater + 20 ml formaldehyde + 50 g NaCl) was carefully stratified underneath the filtered seawater
Postprocessing OIC:
Similiar to the OFOS videos, the photos taken by OIC were georeferenced and converted to Geotiffs using a custom-made software and GDAL.

Preliminary results:
In the following, three exemplary areas will be described, which show three different seafloor settings.

E1
E1 was the first area completely being covered by a multibeam survey. Preliminary results showed that the sea bed was rather flat and homogeneous with depths ranging between 3615 to 3670 m. However, the uniform seafloor led to artifacts in the multibeam signal, which had large effects on the bathymetry. Also, the soft sediment led to errors known as Eric's horn, regularly occurring horn shaped features on both sides of the nadir. Especially in flat regions those outliers change the depth values significantly and need further processing. An OFOS survey was carried out, which underlined the assumption of very homogeneous seafloor and soft sediments.

Eddy site
The eddy region was of particular interest for the benthic projects. Hence, a major focus of seafloor observation was laid on this area, which displayed a marked sea floor topography characterized by the presence of underwater hills and canyon shaped features as well as a pronounced variability in the sidescan back-scatter, which is indicative for seafloor roughness. The combined approach using Multibeam, Sidescan, and OFOS allowed to address these features at different spatial scales and resolution (Fig. 5.2.4.1). Variability in the sediment geochemistry, solute fluxes and microbiological communities (cf. section 5.2.1 to 5.23) might be related to different depositional regime of organic carbon superimposing variabilities in the mass fluxes from the sea surface. Examples of seafloor images in this region are presented in Fig. 5.2.4.2.

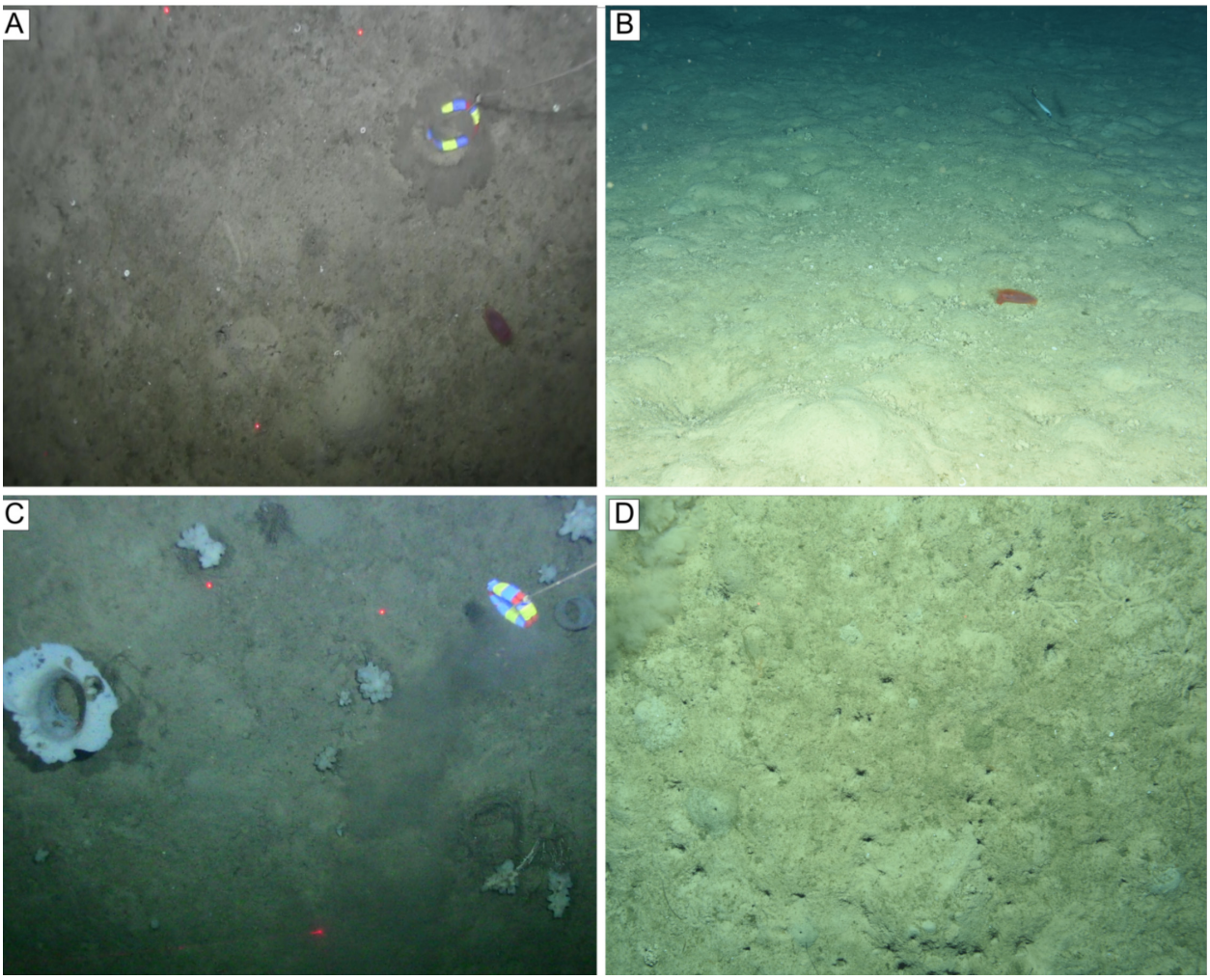

Fig. 5.2.4.2: Underwater images of the seafloor. The blue/red/yellow ring is the pre-weight of the OFOS, hanging 1.5 m below the video sledge. **A**: OFOS dive, close to the BBL lander station. A holothurian, small shells and feeding tracks are visible. **B:** Image from the Ocean Imaging Camera on the BBL lander. The seafloor is characterized by a number of small mounds generated by worms living and feeding inside the sediment. Holothuria (red) are a dominant epifaunal species, which feed on the sediment surface. Grenadier fishes could be observed frequently. **C:** Inside a channel structure white sponges of different sizes were found. As sponges are filter feeders, their occurrence might be related to enhanced particle transport inside the water column. **D:** Numerous holes and feeding mounds suggest high biological activity inside sediments.

Shelf region

The continental shelf region is incised by canyons and debris flow channels, which became especially obvious in the multibeam data. Slopes of the sea floor were very steep from 600 m to 200 m depth within less than one kilometer. The seafloor turned out to be much more active in terms of benthic fauna on the shallow site and reflects increased availability of organic carbon. The OFOS videos and images showed diverse faunal assemblages of fish, crustaceans, and sponges. The permanent need to haul and lower the sledge to avoid collisions with the ground made the hills and trunks actually tangible.

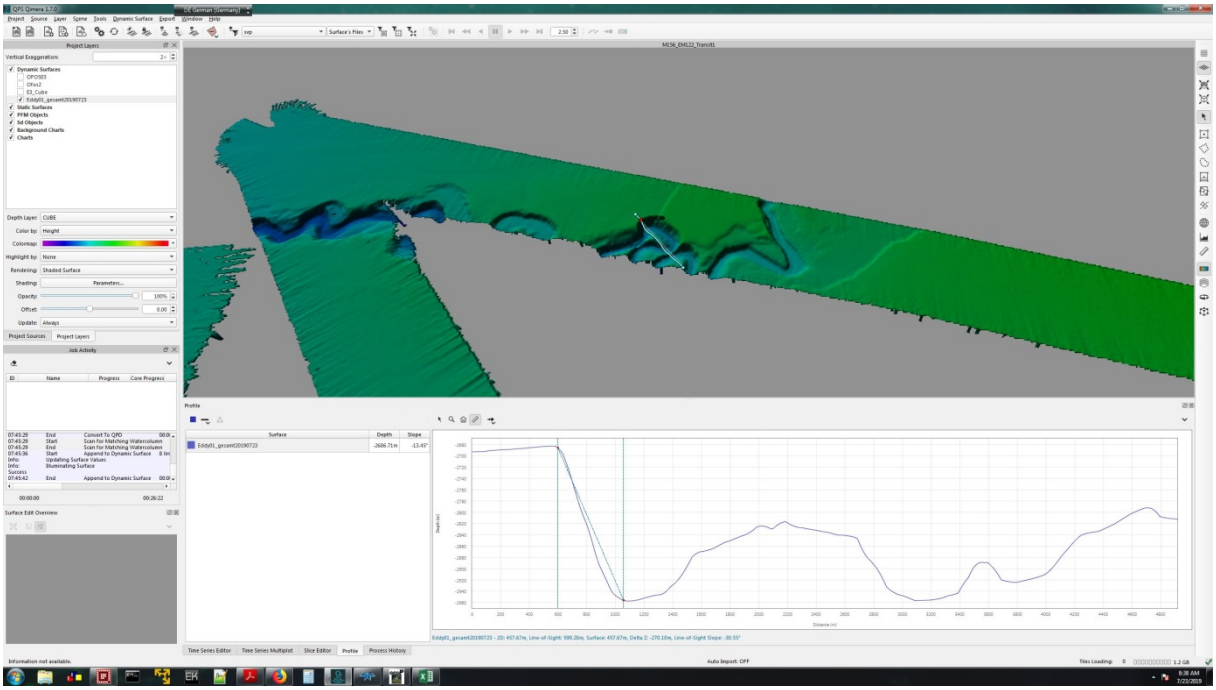

Fig. 5.2.4.3: 3D view of multibeam data and depth profile across a turbidity flow channel structure. The channel side is 270 m high with a slope of 30°.

Seafloor imaging via MBES, DTS and OFOS was successfully conducted. MBES mapping always was the first work inside the research areas. Lander stations were planned based on bathymetry maps.

The MBES data reveals that the seafloor is not always homogeneous, but characterized by steep slopes and channels, especially in the shelf area. Such terrain features can influence local deposition and accumulation of particles at the seabed and hence largely affecting sediment reactivity and exchange of solutes across the sediment water interface. While MBES resolution is limited to ca. 50 m, DTS high resolution backscatter enabled a spatial resolution on meter scales, revealing a high heterogeneity. Using OFOS images and video footage, changes of seafloor flora and fauna could be observed even on centimeter scales, which will become important for the extrapolation of geochemical measurements to wider areas.

5.3 Expected Results

(S. Sommer)

The cruise M156 represents the start of a measurement campaign including two further cruises, altogether addressing the overarching goal to obtain a better quantitative understanding of the dynamics of mesoscale eddies with particular focus to CO_2 source/sink mechanisms and the biological carbon pump in eastern boundary upwelling areas as well as their effects to the oligotrophic periphery including the deep-sea floor. More specifically, during M156 results were obtained to address the following scientific questions and issues:

i. The detailed physical, biological, biogeochemical investigations in combination with seafloor observations along the zonal section at 18°N encompassing shelf and deep-sea area with a maximum depth of ~4200 m provide zonal gradients in pelagic and benthic biogeochemical element cycling, which in turn can potentially be linked with changes in eddy induced primary- and export production.

ii. One major overarching aim of the REEBUS/MOSES projects is to study eddies of different types and maturity. During M156 we were able to successfully sample a cyclonic eddy. Based on these data it is to expect that physical processes of eddy dynamics can be constrained and linked to the specific and biogeochemical and biological processes in the center of the eddy and its periphery with particular regard to CO_2 source and sink mechanisms.
iii. Surprisingly, a red tide formed by the ciliate *Mesodinium rubrum* offshore Mauritania was observed in the area of the cyclonic eddy. We hope that we are able to obtain further indications allowing the assessment whether the occurrence of the red tide can be related to the eddy or whether it represents a completely independent phenomenon.
iv. Underneath the cyclonic eddy benthic carbon cycling and burial has been studied combining in situ flux measurements with porewater/solid-phase geochemistry. We hope that despite the enormous water depth of 2700 to 3000 m the effect of the eddy, if it´s productive at all resulting in a larger carbon rain rate, on benthic carbon availability and cycling can be resolved. The achieved benthic biogeochemical data base will be augmented by further measurements during the third REEBUS/MOSES cruise planned for 2021. During this cruise a Rover will be deployed at the seafloor for up to one year to record a time-series of benthic O_2 fluxes, which will reflect enhanced carbon availability during the passage of productive eddies.
v. From the combined analysis of biogeochemical and microbiological results we expect to get deeper insight into deep-sea benthic microbial communities and their involvement into benthic carbon cycling under various depositional regimes of particulate organic carbon.
vi. Deposition of particulate organic carbon on the seafloor is largely affected by seafloor topography and activity of burrowing fauna, introducing variability into in-situ flux measurements of organic carbon degradation. It is to expect that this variability can be better constrained by careful analysis of the in-situ fluxes and sediment biogeochemistry in relation to data obtained during seafloor observation. This topic will be a major topic during the third cruise MOSES Eddy Study III.

6 Ship´s Meteorological Station

The 3rd of July 2019 at 18:30 the research vessel METEOR left the harbour of Mindelo / Sao Vicente – Cape Verde. During the entire expedition, the working area, which was extending from Cape Verde to Mauritania along 18°N, was located at the southeastern flank of an extended high pressure system over the central North Atlantic Ocean. At the start of the journey the north-east trade wind blew with 4 to 5 Bft. While leaving the shelter of the island, the significant wave height increased to 2.5 m, mainly due to the swell arriving from Northeast. Due to the proximity of the working area to the West African coast Saharan dust impaired the visibility during the entire expedition. On 8th of July the sea started to slowly decrease to 1.5 m. At the 10th of July a temporarily strengthening of the north-east trade wind of up to 6 Bft resulted in a short-term increase of the sea state to 2.5 m. Moving eastward RV METEOR gradually was influenced by a thermal low with multiple centers over North Africa. Blowing with 4 to 5 Bft, the wind slowly backed and shifted on 13th of July to northern directions. On the 16th of July, for the first time of this expedition the wind dropped to 1 to 2 Bft for two days.
On the 19th of July, the research area was shifted 60 nm to the north for one day. The pressure gradient between the Azores high pressure system and the thermal low over West Africa intensified, whereby the north-east trade wind increased to 6 Bft with gusts 8 Bft and the sea state rose again to 2.5 m. Another wind field reached RV METEOR on 22nd July. The wind went up to 7 Bft and the sea rose up to 3 m. With the decrease of wind speed to 3 to 4 Bft one day later, the sea state gradually eased back to 1.5 m. Furthermore, on the 23rd of July the peak of Saharan dust during this journey was reached, leading to a visibility reduction to 7 km.

From 26th to 28th July the research of R/V METEOR was conducted at the easternmost point of the working area. The wind direction shifted to Northwest to West with 4 Bft or less. The sea state dropped to 1 m. On the 27th of July, the so far dominating swell from North turned to Northwest and during one day an additional swell from southwestern directions joined.
On Tuesday the 30th of July, the transit back to Mindelo started. The wind blew with 4 to 5 Bft with a wind direction from Northwest at first, which shifted to North and later to Northeast while travelling west. The sea state slightly increased to 2.0 m and the northerly swell prevailed again.
On 1st of August around 08:00 RV Meteor reached the harbour of Mindelo.
German Weather Service, marine weather office on board of R/V METEOR, Wft Martin Stelzner, 1st August 2019 Translation J. Wenzel

7 Station List M156

Station #	Date	Time (UTC)	Gear #	Latitude	Longitude	Depth (m)	Remarks
M156-1	04.07.19	03:34	CTD 01	17°59.994'N	24°20.022'W	3680	Nutrients
M156-2	04.07.19	07:34	MSC 01	18°00.005'N	24°20.010'W	3694	
M156-3	04.07.19	07:58	CTD 02	17°59.996'N	24°20.024'W	3696	similar pos. as CTD 01
M156-4	04.07.19	09:22	MUC 01	18°00.004'N	24°20.011'W	3694	2 liner empty
M156-5	04.07.19	12:38	MUC 02	18°00.001'N	24°20.011'W	3714	
M156-6	04.07.19	19:27	BIGO-II 01	18°00.003'N	24°20.010'W	3718	Deployment Problem Telemetry
M156-7	05.07.19	05:56	CTD 03	17°59.966'N	23°36.522'W	3633	Nutrients
M156-8	05.07.19	11:00	MBES 01				
M156-9	05.07.19	18:28	MSS 01	18°00.005'N	24°20.012'W	3716	4 profiles
M156-10	05.07.19	20:00	OFOS 1/2[a]				On deck: 06:35 UTC
M156-11	06.07.19	09:28	CTD 04	17°35.000'N	24°17.000'W	3590	Nutrients
M156-12	06.07.19	14:30	MSC 02	17°59.996'N	24°20.051'W	3714	
M156-13	07.07.19	03:39	CTD 05	17°59.976'N	21°59.969'W	3312	
M156-14	07.07.19	04:55	MSS 02	18°00.062'N	21°59.996'W	3312	Aborted, due to winch
M156-15	07.07.19	05:36	CTD 06	18°00.08'N	21°59.984'W	3315	cable damage
M156-16	07.07.19	09:07	MUC 03	17°59.998'N	22°00.003'W	3315	MUC hitherto op. Prototype-Tememetry
M156-17	07.07.19	14:12	BIGO-II 02	17°59.997'N	22°00.003'W	3559	Deployment, Releaser Problem
M156-18	07.07.19	18:42	MSC 03	18°00.001'N	22°00.005'W	3313	
M156-19	07.07.19	20:39	BIGO-II 03	17°59.999'N	22°00.004'W	3312	Deployment E2
M156-20	07.07.19	23:45	MBES 02				
M156-21	08.07.19	04:58	CTD 07	18°00.016'N	22°47.077'W	3432	Nutrients
M156-22	08.07.19	10:20	CTD 08	17°59.996'N	22°00.008'W	3311	Nutrients
M156-23	08.07.19	13:12	MSC 04	17°59.998'N	22°00.008'W	3315	
M156-24	08.07.19	13:32	MSS 03	17°59.901'N	22°00.014'W	3316	3 profiles
M156-25	08.07.19	15:05	OFOS 03				USBL was used, but position not reliable
M156-26	09.07.19	05:09	CTD 09	17°60.000'N	21°08.005'W	3142	Samples of O2 & Nutrients
M156-27	09.07.19	10:00	MBES 03				
M156-28	09.07.19	13:30	BIGO-II 03	17°59.722'N	22°00.534'W	3316	Recovery
M156-29	10.07.19	15:27	BIGO-II 04	21°10.004'N	20°55.004'W	4195	Deployment failed, releaser
M156-30	10.07.19	22:06	BIGO-II 05	21°10.005'N	20°55.004'W	4197	Deployment, releaser changed CB
M156-31	11.07.19	02:00	MBES 04				
M156-32	11.07.19	09:00	CTD 10	21°26.478'N	21°44.495'W	4410	
M156-33	11.07.19	16:38	OFOS 04				Posidonia 4
M156-34	12.07.19	05:39	CTD 11	21°09.971'N	20°55.019'W	4186	
M156-35	12.07.19	07:25	MSS 04	21°09.978' N	20°55.016'W	4185	3 profiles
M156-36	12.07.19	08:15	MSC 05	21°10.035'N	20°54.982'W	4186	
M156-37	12.07.19	09:00	CTD 12	21°10.037'N	20°54.983'W	4169	Nutrients
M156-38	12.07.19	12:11	MUC 04	21°10.007'N	20°55.004'W	4186	
M156-39	12.07.19	15:21	BIGO-II 05	21°10'N	20°55'W	4186	Recovery
M156-40	13.07.19	11:13	MUC 05	18°00.002'N	19°33.006'W	3228	
M156-41	13.07.19	15:40	BIGO-II 06	18°00.001'N	19°33.006'W	3226	Deployment E6
M156-42	13.07.19	17:25	MBES 05				
M156-43	14.07.19	05:01	CTD 13	17°59.985'N	19°33.005'W	3227	
M156-44	14.07.19	06:05	MSS 05	18°00.066'N	19°32.973'W	3227	3 profiles
M156-45	14.07.19	07:21	MSC 06	18°00.076'N	19°32.933'W	3226	On deck: 07:57 UTC
M156-46	14.07.19	08:11	CTD 14	18°00.076'N	19°33.012'W	3227	Nutrients
M156-47	14.07.19	10:40	WG 01	18°00.163'N	19°32.907'W	3226	Deployment
M156-48	14.07.19	15:00	OFOS 05				
M156-49	14.07.19	23:19	LD 01	18°01.153'N	19°32.766'W	3226	Deployment
M156-50	15.07.19	04:09	CTD 15	18°00.002'N	20°18,012'W	3169	SensorsCalibration, Nutrients
M156-51	15.07.19	09:45	MSC 07	17°59.982'N	19°33.030'W	3228	On deck: 09:53 UTC
M156-52	15.07.19	11:57	LD 01	17°56.442'N	19°30.362'W	3223	Recovery
M156-53	15.07.19	13:33	BIGO-II 06	17°59.529'N	19°33.159'W	3225	Recovery
M156-54	15.07.19	17:35	ADCP				Sidescan reference
M156-55	16.07.19	13:30	SES 01				

Station #	Date	Time (UTC)	Gear #	Latitude	Longitude	Depth (m)	Remarks
M156-56	17.07.19	19:38	CTD 16	18°17.611'N	19°06.740'W	3115	
M156-57	17.07.19	20:30	MSC 08	18°17.596'N	19°06.806'W	3116	On deck 20:50 UTC
M156-58	17.07.19	20:51	CTD 17	18°17.599'N	19°06.790'W	3214	Nutrients
M156-59	17.07.19	23:54	CTD 18	18°17.602'N	18°49.571'W	3049	Nutrients
M156-60	18.07.19	02:44	CTD 19	18°17.586'N	18°41.477'W	3029	Nutrients
M156-61	18.07.19	05:27	CTD 20	18°17.573'N	18°21.989'W	3029	Nutrients
M156-62	18.07.19	08:00	MUC 06	18°16.911'N	18°11.526'W	2833	
M156-63	18.07.19	14:01	BIGO-II 07	18°16.908'N	18°11.528'W	2833	Deployment (Gas-Releaser)
M156-64	18.07.19	18:04	MSS 07[b]	18°16.649'N	18°14.636'W	2843	3 Profiles
M156-65	18.07.19	19:30	MSC 09	18°17.534'N	18°15.345'W	2856	On deck: 19:35 UTC
M156-66	18.07.19	19:49	CTD 21	18°17.543'N	18°15.309'W	2839	
M156-67	18.07.19	23:43	CTD 22	18°17.587'N	18°32.402'W	2974	Protozoa
M156-68	19.07.19	00:13	MSS 08	18°17.641'N	18°32.397'W	2974	
M156-69	19.07.19	01:27	CTD 23	18°17.572'N	18°32.394'W	2973	
M156-70	19.07.19	02:14	CTD 24	18°17.574'N	18°32.390'W	2974	Nutrients
M156-71	19.07.19	10:25	MUC 07	19°19.756'N	19°45.263'W	2877	
M156-72	19.07.19	14:42	BIGO-I 01	19°19.804'N	18°45.208'W	2874	Deployment
M156-73	19.07.19	20:14	MSS 09	19°26.321'N	18°22.046'W	3294	3 Profiles
M156-74	19.07.19	21:30	MSC 10	19°26.325'N	18°22.208'W	3035	On deck: 21:40 UTC
M156-75	19.07.19	21:57	CTD 25	19°26.35'N	18°22.206'W	2576	Nutrients
M156-76	20.07.19	01:03	MSS 10	19°09.227'N	18°22.040'W	2673	3 Profiles
M156-77	20.07.19	01:57	CTD 26	19°09.798'N	18°22.463'W	2678	Nutrients
M156-78	20.07.19	04:40	CTD 27	18°51.913'N	18°22.086'W	2790	Nutrients
M156-79	20.07.19	07:28	CTD 28	18°34.771'N	18°21.989'W	2817	Nutrients
M156-80	20.07.19	08:40	MSC 11	18°34.807'N	18°21.988'W	2819	On deck: 08:55 UTC
M156-81	20.07.19	09:00	MSS 11	18°34.833'N	18°21.981'W	2817	3 Profiles
M156-82	20.07.19	11:42	BIGO-II 07	18°16.568'N	18°11.616'W	2835	Recovery
M156-83	20.07.19	15:10	OFOS 06				
Red Tide	20.07.19	18:37		18°16.928'N	18°11.317'W	2830	water sampling bucket
M156-84	20.07.19	20:20	OFOS 07				
M156-85	21.07.19	13:30	BIGO-I 01	19°19.428'N	18°45.382'W	2876	Recovery
M156-86	21.07.19	15:15	Lightsensor 01	19°19.843'N	18°45.321'W	3122	RAMSES
M156-87	21.07.19	19:03	CTD 29	19°09.197'N	18°05.18'W	2497	Nutrients
M156-88	21.07.19	20:20	MSC 12	19°09.198'N	18°05.021'W	2500	On deck: 20:26 UTC
M156-89	21.07.19	21:36	MSS 12	18°59.110'N	18°05.082'W	2614	2 Profiles
M156-90	21.07.19	22:45	CTD 30	19°00.063'N	18°05.028'W	2596	Nutrients
M156-91	22.07.19	00:42	CTD 31	18°51.967'N	18°04.981'W	2626	Nutrients
M156-92	22.07.19	02:53	MSS 13	18°42.297'N	18°05.136'W	2673	3 Profiles
M156-93	22.07.19	03:57	CTD 32	18°43.428'N	18°05.015'W	2663	Nutrients
M156-94	22.07.19	05:59	CTD 33	18°34.783'N	18°04.996'W	2717	Nutrients
M156-95	22.07.19	07:15	MSC 13	18°34.784'N	18°04.996'W	2717	On deck: 07:24 UTC
M156-96	22.07.19	07:31	MSS 14	18°34.838'N	18°04.996'W	2719	3 Profiles
M156-97	22.07.19	08:30	CTD 34	18°34.780'N	18°04.954'W	3790	
M156-98	22.07.19	09:15	CTD 35	18°34.782'N	18°04.953'W	2699	
M156-99	22.07.19	12:15	MSC 14	18°34.782'N	18°04.953'W	2724	On deck: 12:25 UTC
M156-100	22.07.19	14:39	BIGO-I 02	18°14.165'N	18°09.296'W	2823	Deployment, failed
M156-101	22.07.19	20:47	BBL 01	18°05.847'N	17°58.821'W	2829	Deployment
M156-102	22.07.19	23:56	MBES 06				
M156-103	23.07.19	09:35	BIGO-I 03	18°14.238'N	18°09.447'W	2820	Deployment
M156-104	23.07.19	15:13	BIGO-II 08	17°46.198'N	18°03.200'W	2943	Deployment
M156-105	23.07.19	18:53	MSS 15	17°50.925'N	18°04.737'W	2943	
M156-106	23.07.19	19:53	CTD 36	17°51.762'N	18°05.047'W	2874	Nutrients
M156-107	23.07.19	22:33	CTD 37	17°59.818'N	18°04.933'W	2871	Nutrients
M156-108	23.07.19	23:40	MSC 15	18°00.234'N	18°04.965'W	2869	On deck: 23:46 UTC
M156-109	24.07.19	00:33	MSS 17	18°00.259'N	18°04.962'W	2869	3 Prof., MSS16 not existing
M156-110	24.07.19	02:21	MSS 18	18°07.973'N	18°05.000'W	2660	3 Profiles at about 220dbar
M156-111	24.07.19	03:27	CTD 38	18°08.980'N	18°05.002'W	2600	Nutrients
M156-112	24.07.19	05:34	MSS 19	18°17.440'N	18°05.002'W	2791	
M156-113	24.07.19	06:33	CTD 39	18°17.603'N	18°05.021'W	2790	Nutrients
M156-114	24.07.19	08:36	CTD 40	18°26.167'N	18°04.990'W	2768	Nutrients
M156-115	24.07.19	10:49	LD 02	18°34.785'N	18°05.041'W	2717	Deployment
M156-116	24.07.19	11:49	Glider 01	18°35.054'N	18°05.343'W	2717	Deployment
M156-117	24.07.19	13:40	MUC 08	18°34.800'N	18°05.000'W	2717	
M156-118	24.07.19	17:32	BIGO-I 03	18°13.818'N	18°09.321'W	2820	Recovery
M156-119	24.07.19	20:22	OFOS 08				

Station #	Date	Time (UTC)	Gear #	Latitude	Longitude	Depth (m)	Remarks
M156-120	25.07.19	10:00	MUC 09	17°46.117'N	18°03.184'W	2958	
M156-121	25.07.19	13:32	BIGO-II 08	17°46.102'N	18°02.511'W	2966	Recovery
M156-122	25.07.19	20:01	BIGO-I 04	18°34.742'N	18°05.007'W	2715	Deployment
M156-123	26.07.19	00:25	LD 02	18°36.485'N	17°58.127'W	2654	Recovery
M156-124	26.07.19	01:17	MSS 20	18°33.875'N	17°57.813'W	2675	
M156-125	26.07.19	02:12	CTD 41	18°34.797'N	17°57.999'W	2668	Nutrients
M156-126	26.07.19	03:30	MSC 16	18°34.796'N	17°57.999'W	2667	On deck: 03:48 UTC
M156-127	26.07.19	04:45	MSS 21	18°33.920'N	17°49.285'W	2599	
M156-128	26.07.19	05:50	CTD 42	18°34.878'N	17°49.331'W	2597	Nutrients
M156-129	26.07.19	07:59	MSS 22	18°34.018'N	17°40.737'W	2509	
M156-130	26.07.19	08:55	CTD 43	18°34.843'N	17°40.788'W	2504	Nutrients
M156-131	26.07.19	11:16	MSS 23	18°33.872'N	17°32.166'W	2428	
M156-132	26.07.19	12:07	CTD 44	18°34.831'N	17°32.132'W	2418	Nutrients
M156-133	26.07.19	16:11	BIGO-I 04	18°34.631'N	18°04.778'W	2714	Recovery, Eddy center
M156-134	26.07.19	21:03	MSS 24	18°33.842'N	17°23.586'W	2305	
M156-135	26.07.19	22:04	CTD 45	18°34.793'N	17°23.572'W	2346	Nutrients
M156-136	27.07.19	00:11	MSS 25	18°33.748'N	17°15.054'W	2124	
M156-137	27.07.19	01:15	CTD 46	18°34.800'N	17°15.031'W	2146	Nutrients
M156-138	27.07.19	07:00	CTD 47	18°09.960'N	16°30.972'W	182	Nutrients
M156-139	27.07.19	07:40	MSC 17	18°09.979'N	16°30.984'W	182	On deck: 08:00 UTC
M156-140	27.07.19	09:15	MUC 10	18°10.268'N	16°31.028'W	182	
M156-141	27.07.19	13:19	BIGO-II 09	18°10.268'N	16°31.027'W	181	Deployment
M156-142	27.07.19	16:59	CTD 48	18°34.826'N	16°23.431'W	58	Nutrients
M156-143	27.07.19	18:07	CTD 49	18°34.943'N	16°31.988'W	130	Nutrients
M156-144	27.07.19	19:28	MSS 26	18°34.727'N	16°40.624'W	356	
M156-145	27.07.19	20:30	CTD 50	18°34.788'N	16°40.566'W	353	Nutrients
M156-146	27.07.19	22:13	MSS 27	18°35.897'N	16°49.216'W	832	
M156-147	27.07.19	23:23	CTD 51	18°34.794'N	16°49.182'W	890	Nutrients
M156-148	28.07.19	01:15	MSS 28	18°35.867'N	16°57.700'W	588	
M156-149	28.07.19	02:11	CTD 52	18°34.953'N	16°57.720'W	1605	Nutrients
M156-150	28.07.19	04:19	MSS 29	18°34.808'N	17°05.670'W	1841	
M156-151	28.07.19	06:26	CTD 53	18°34.783'N	17°06.358'W	1877	Nutrients
M156-152	28.07.19	07:35	MSC 18	18°34.793'N	17°06.374'W	1878	On deck: 07:40 UTC
M156-153	28.07.19	13:13	Glider 01	18°41.326'N	16°59.438'W	1256	Recovery
M156-154	28.07.19	13:34	Lightsensor 02	18°41.327'N	16°59.347'W	1253	RAMSES
M156-155	28.07.19	19:35	CTD 54	17°59.994'N	17°26.976'W	2448	Nutrients
M156-156	28.07.19	20:54	MSC 19	17°59.994'N	17°26.976'W	2448	On deck: 20:58 UTC
M156-157	28.07.19	22:37	CTD 55	17°59.990'N	17°11.167'W	2045	Nutrients
M156-158	29.07.19	01:05	CTD 56	17°59.971'N	16°55.393'W	1530	Nutrients
M156-159	29.07.19	02:22	SVP Drifter 01	17°59.866'N	16°55.027'W	1502	
M156-160	29.07.19	03:43	CTD 57	17°59.972'N	16°39.529'W	694	Nutrients
M156-161	29.07.19	05:49	CTD 58	18°10.244'N	16°30.934'W	181	
M156-162	29.07.19	06:45	MSC 20	18°10.246'N	16°30.933'W	181	On deck: 06:52 UTC
M156-163	29.07.19	09:04	BIGO-II 09	18°10.139'N	16°30.794'W	176	Recovery
M156-164	29.07.19	11:45	OFOS 09				
M156-165	29.07.19	15:19	CTD 59	17°59.980'N	16°31.994'W	417	Nutrients
M156-166 & 167	29.07.19	16:30	OFOS 10 a/b				
M156-168	29.07.19	23:06	MBES 07				
M156-169	30.07.19	13:37	Lightsensor 03	18°05.514'N	17°58.764'W	2832	RAMSES
M156-170	30.07.19	14:13	BBL 01	18°05.516'N	17°58.764'W	2830	Recovery
M156-171	31.07.19	13:05	Lightsensor 04	18°05.350'N	22°06.349'W	3316	RAMSES On deck: 13:19 UTC

[a] OFOS survey was splitted in two video data files. USBL was used, but position not reliable.
[b] MSS 06 aborted prior to deployment, hence not listed in the station list.

Abbreviations of the different gears/Measured parameters

Water column

ADCP: ship board current measurements
CTD: (CTD watersampling rosette), physical properties, nutrients
Glider: Physical properties, turbulence, O_2, nitrate
LD: Lagrangian Surface Drifter, biogeochemical properties
Light Sensor: RAMSES, irradiance
MSC: Marine Snow Catcher, particles for biogeochemical analyses
MSS: (Microstructure Sensor): Physical properties and turbulence
SVP Drifter

WG: Waveglider, physical and biogeochemical properties

Benthos
BBL: Benthic Boundary Layer Lander: Seafloor imaging, physical properties, sediment trap
BIGO-1/-2: Biogeochemical Observatory: In situ element fluxes, sediments for biogeochemistry
MBES: Multibeam bathymetrical measurements
MUC: Multiple corer video-guided, sediments for geochemistry and microbiology
OFOS: Ocean Floor Observation System, towed camera system for sea floor imaging
SES: Sidescan, seafloor monitoring

8 Data and Sample Storage and Availability

The data were collected within the REEBUS project (BMBF) and the MOSES project (HGF). The data management is handled by the GEOMAR data management team. Data sharing and exchange will take place within the Ocean Science Information System (OSIS-Kiel) hosted at GEOMAR. In a first phase data are only available to the project members. After a two year proprietary time the data management team will publish these data by dissemination to national and international data archives, i.e. the data will be submitted to PANGAEA no later than 2021. Digital object identifiers (DOIs) are automatically assigned to data sets archived in the World Data Centre PANGAEA (Data Publisher for Earth & Environmental Science) making them publically retrievable, citeable and reusable for the future. All metadata are immediately available publically via the following link pointing to OSIS-Kiel in the GEOMAR data management portal (https://portal.geomar.de/metadata/leg/show/348695). In addition, the portal provides a single downloadable KML formatted file (https://portal.geomar.de/metadata/leg/kmlexport/348695), which retrieves and combines up-to-date cruise (M156) related information, links to restricted data and to published data for visualization e.g. in GoogleEarth. In adherence to the MOSES Data Policy, basic campaign data, sensor metadata as well as metadata about collected data sets (including links to OSIS and PANGAEA) will be made publically available using the MOSES data portal. This does not affect the two-year proprietary use period for collected data, since only metadata will be published at the MOSES Portal. To facilitate this, deployed sensors and devices will be registered in a sensor repository (sensor.awi.de) and campaign metadata is recorded in the MOSES Datamanagement Plan Tool (https://moses-dmp.gfz-potsdam.de/).

Table 8.1. Overview of data availability. For data storage and availability please see text above. Free access of data will become available at December 2021

Data type	Contact person: Name, Institute, e-mail
Water column	
CTD, ADCP	M. Dengler, GEOMAR, mdengler@geomar.de
Microstructure CTD	M. Dengler, GEOMAR, mdengler@geomar.de
Glider	M. Dengler, GEOMAR, mdengler@geomar.de
Water column nutrients (CTD Rosette)	S. Sommer, GEOMAR, ssommer@geomar.de
Biogeochemistry	K. Becker, A. Engel, GEOMAR, aengel@geomar.de
Protist Biology	H.-W. Breiner, T. Stoeck, TUKL, breiner@rhrk.uni-kl.de
Waveglider, Lagrangian Drifter	M. Paulsen, B. Fiedler, A. Körtzinger, GEOMAR, akörtzinger@geomar.de

Benthos	
Porewater geochemistry	A. Dale, GEOMAR, adale@geomar.de
Benthic in situ fluxes	S. Sommer, GEOMAR, ssommer@geomar.de
Sea floor observation	M. Kampmeier, J. Greinert, GEOMAR, jgreinert@geomar.de
Microbiology	N. Adam, M. Perner GEOMAR, mperner@geomar.de

9 Acknowledgements

We very much thank Captain Rainer Hammacher, the officers and the entire crew of RV METEOR for their excellent support. They created a very professional working environment and contributed a lot to the success of this cruise. The friendly atmosphere aboard is greatly acknowledged. We thank the Ministère des Pêches et de l'Ecconomie Maritime (République Islamique de Mauritanie) and the Instituto Maritimo Portuàrio-IMP (Cabo Verde) for their support and the allowance to conduct research in Mauritanian and Cape Verdian waters. We very much like to acknowledge the support of the German Ministry of Foreign Affairs.
We would also like to express our gratitude to the Geschäftsstelle des Gutachterpanels Forschungsschiffe (GPF) and the Leitstelle Deutsche Forschungsschiffe (Hamburg) for their valuable support. The ship time of RV METEOR and financial support for the logistics of the cruise was kindly provided by the German Research Council, DFG. The project REEBUS is funded by the German Ministry for Education and Research, BMBF.

10 References

Alldredge, A.L., Passow, U., Logan, B.E., 1993 The abundance and significance of a class of large, transparent organic particles in the ocean. Deep-Sea Res. Part I 40, 1131–1140.

Azam, F., Fenchel, T., Field, J., Gray, J., Meyer-Reil, L., Thingstad, F., 1983 The Ecological Role of Water-Column Microbes in the Sea. Mar. Ecol. Prog. Ser. 10, 257–263.

Becker, K.W., Elling, F.J., Schröder, J.M., Lipp, J.S., Goldhammer, T., Zabel, M., Elvert, M., Overmann, J., Hinrichs, K.-U., 2018 Isoprenoid quinones resolve the stratification of microbial redox processes in a biogeochemical continuum from the photic zone to deep anoxic sediments of the Black Sea. Appl. Environ. Microbiol. 84(10), e02736-17.

Brannigan, L., 2016 Intense submesoscale upwelling in anticyclonic eddies. Geophysical Research Letters 43(7), 3360–3369.

Busch, K., Endres, S., Iversen, M.H., Michels, J., Nöthig, E.-M., Engel A., 2017 Bacterial Colonization and Vertical Distribution of Marine Gel Particles TEP and CSP in the Arctic Fram Strait. Front. Mar. Sci. 4, 166.

Cisternas-Novoa, C., Lee, C., Engel A., 2015. Transparent exopolymer particles TEP and Coomassie stainable particles CSP: Differences between their origin and vertical distributions in the ocean. Mar. Chem. 175, 56–71.

Dale, A. W., Sommer, S., Ryabenko, E., Noffke, A., Bohlen, L., Wallmann, K., Stolpovsky, K., Greinert, J., Pfannkuche, O., 2014 Benthic nitrogen fluxes and fractionation of nitrate in the

Mauritanian oxygen minimum zone (Eastern Tropical North Atlantic). Geochim. Cosmochim Acta 134, 234-256.

Dhakar, S. P., Burdige, D. J., 1996 A coupled, non-linear, steady-state model for early diagenetic processes in pelagic sediments. Am J Sci 296,296-330.

Dickson, A. G., Sabine, C. L., Christian, J. R. (Eds.), 2007 Guide to Best Practices for Ocean CO2 Measurements. PICES Special Publication 3.

Engel, A., 2009 Determination of marine gel particles. In Practical guidelines for the analysis of seawater. CRC Press. pp. 137–154.

Engel, A., Galgani, L., 2016 The organic sea-surface microlayer in the upwelling region off the coast of Peru and potential implications for air-sea exchange processes. Biogeosciences 13, 989–1007.

Engel, A., Händel, N., 2011 A novel protocol for determining the concentration and composition of sugars in particulate and in high molecular weight dissolved organic matter HMW-DOM in seawater. Mar. Chem. 127, 180–191.

Fiedler, B., Grundle, D., Schütte, F., Karstensen, J., Löscher, C.R., Hauss, H., Wagner, H., Loginova, A., Kiko, R., Silva, P., Körtzinger, A., 2016 Oxygen utilization and downward carbon flux in an oxygen-depleted eddy in the Eastern Tropical North Atlantic. Biogeosciences 13, 5633-5647.

Fischer, G., Romero, O., Merkel, U., Donner, B., Iversen, M., Nowald, N., Ratmeyer, V., Ruhland, G., Klann, M., Wefer, G., 2016 Deep ocean mass fluxes in the coastal upwelling off Mauritania from 1988 to 2012: variability on seasonal to decadal timescales. Biogeosciences 13, 3071-3090.

Gargas, E. 1975. A manual for phytoplankton primary production studies in the Baltic. Baltic Marine Biologists Publ. no. 2. Danish Water Quality Institute, Horsholm.

Grasshof, K., Kremling, K., Ehrardt, M. 1999 Methods of seawater analysis; 3. compl. rev. and ext. ed.

Hauss, H., Christiansen, S., Schütte, F., Kiko, R., Edvam Lima, M., Rodrigues, E., Karstensen, J., Löscher, C.R., Körtzinger, A., Fiedler, B., 2016 Dead zone or oasis in the open ocean? Zooplankton distribution and migration in low-oxygen modewater eddies. Biogeosciences, 13, 1977-1989.

Ivanenkov V. N., Lyakhin Y., 1978. Determination of total alkalinity in seawater. In Methods of Hydrochemical Investigations in the Ocean (eds. O. K. Bordovsky and V. N. Ivanenkov). Nauka Publishing House, pp. 110–114.

Karstensen, J., Schütte, F., Pietri, A., Krahmann, G., Fiedler, B., Grundle, D., Hauss, H., Körtzinger, A. et al., 2017 Upwelling and isolation in oxygen-depleted anticyclonic modewater eddies and implications for nitrate cycling. Biogeosciences,14, 2167-2181, doi:10.5194/bg-14-2167-2017, 2017.

Karstensen, J., Fiedler, B., Schütte, F., Brandt, P., Körtzinger, A., Fischer, G., Zantopp, R., Hahn, J., Visbeck, M., Wallace, D., 2015 Open ocean dead-zone in the tropical North Atlantic Ocean. Biogeosciences,12, 2597-2605.

Kirchman, D., K'nees, E., Hodson, R., 1985. Leucine incorporation and its potential as a measure of protein synthesis by bacteria in natural aquatic systems. Appl. Environ. Microbiol. 49, 599–607.

Klein, P., Lapeyre, G., 2009 The oceanic vertical pump induced by mesoscale and submesoscale turbulence. Ann. Rev. Mar. Sci. 1: 351-375.

Kunze, E., Schmitt, R.W., Toole, J.M. (1995). The energy balance in a warm-core ring's near-inertial critical layer. J. Phys. Oceanogr. 25, 942-957.

Lindroth, P., Mopper, K., 1979 High performance liquid chromatographic determination of subpicomole amounts of amino acids by precolumn fluorescence derivatization with o-phthaldialdehyde. Anal. Chem. 51, 1667–1674.

Loginova, A.N., Thomsen, S., Engel A., 2016 Chromophoric and fluorescent dissolved organic matter in and above the oxygen minimum zone off Peru. J. Geophys. Res. Ocean 121, 7973–7990.

Long, R.A., Azam, F., 1996 Abundant protein-containing particles in the sea. Aquat. Microb. Ecol. 10, 213–221.

Löscher, C.R., Fischer, M.A., Neulinger, S.C., Fiedler, B., Philippi, M., Schütte, F., Singh, A., Hauss, H., Karstensen, J., Körtzinger, A., Künzel, S., Schmitz, R.A., 2015 Hidden biosphere in an oxygen-deficient Atlantic open-ocean eddy: future implications of ocean deoxygenation on primary production in the eastern tropical North Atlantic. Biogeosciences, 12, 7467-7482.

Nielsen, E.S., 1952 The use of radioactive carbon (C14) for measuring organic production in the sea. J. Cons. 18, 117–140.

Omand, M.M., D'Asaro, E.A., Lee, C.M., Perry, M.J., Briggs, N., Cetinić, I., Mahadevan A., 2015 Eddy-driven subduction exports particulate organic carbon from the spring bloom. Science 348(6231), 222–225.

Scholz, F., Löscher, C. R., Fiskal, A., Sommer, S. Hensen. C., Lomnitz, U., Wuttig, K., Göttlicher, J., Kosse, E., Steininger, R., Canfield, D. E., 2016 Nitrate-dependent iron oxidation limits iron transport in anoxic ocean regions. Earth Planet. Sci. Lett. 454, 272-281.

Smith, D.C., Azam, F., 1992 A simple, economical method for measuring bacterial protein synthesis rates in seawater using 3H-leucine. Mar. Microb. Food Webs 6, 107–114.

Sommer. S., Clemens, D., Yücel, M., Pfannkuche, O., Hall, P.O.J., Almroth-Rosell, E., Schulz-Vogt, H.N., Dale, A.W., 2017 Major bottom water ventilation events do not significantly reduce basin-wide benthic N and P release in the Eastern Gotland Basin (Baltic Sea). Front. Mar. Sci. 4,18. doi: 10.3389/fmars.2017.00018

Sommer, S., Dengler, T., Treude, T., 2015 Benthic element cycling, fluxes and transport of solutes across the benthic boundary layer in the Mauritanian oxygen minimum zone, (SFB754) – Cruise No. M107 – May 30 – July 03, 2014 –Fortaleza (Brasil) – Las Palmas (Spain). Meteor Berichte, M107, 54 pp., DFG-Senatskommission für Ozeanographie.

Sommer, S., Gier, J., Treude, T., Lomnitz, U., Dengler, M., Cardich, J., Dale, A.W., 2016 Depletion of oxygen, nitrate and nitrite in the Peruvian oxygen minimum zone cause an imbalance of benthic nitrogen fluxes. Deep-Sea Res I 112,113-122.

Sommer, S., Linke, P., Pfannkuche, O., Schleicher, T., Schneider v. Deimling, J., Reitz, A., Haeckel, M., Flögel, S., Hensen, C., 2009 Seabed methane emissions and the habitat of frenulate tubeworms on the Captain Arutyunov mud volcano (Gulf of Cadiz). Mar Ecol Prog Ser 382, 69-86.

Sugimura, Y., Suzuki, Y., 1988 A high-temperature catalytic oxidation method for the determination of non-volatile dissolved organic carbon in seawater by direct injection of a liquid sample. Mar. Chem. 24, 105–131.

Vikström, K., Tengberg, A., Wikner, J., 2019 Improved accuracy of optode-based oxygen consumption measurements by removal of system drift and nonlinear derivation. *Limnol. Oceanogr. Methods* 17, 179–189.

Wenzhöfer, F., Glud, R.H., 2002 Benthic carbon mineralization in the Atlantic: a synthesis based on in situ data from the last decade. Deep-Sea Research I 49, 1255-1279.

Wörmer, L., Lipp, J.S., Schröder, J.M., Hinrichs K.-U., 2013 Application of two new LC–ESI–MS methods for improved detection of intact polar lipids IPLs in environmental samples. Org. Geochem. 59, 10–21.

Zhang, Z., Wang, W., Qui, B., 2014 Oceanic mass transport by mesoscale eddies. Science 345, 322-324.